 doi:10.20944/preprints201906.0288.v1

Cancer: Strange Attractors and Complexity

Abicumaran Uthamacumaran

Concordia University
a_utham@live.concordia.ca

Cancer is a complex adaptive ecosystem and remains the lead cause of disease-related death in pediatric patients in North America. Machine learning, Network science, Fluid dynamics and Quantum Mechanics are hereby discussed as tools to advance oncology and cancer reprogramming. The fluid dynamics of cell-fate transitions, cancer pattern formation and invasion are reviewed in this paper. Cancer cell decision-making is investigated through dynamical systems and complexity theory. A fluid-dynamics grid-scheme based Deep Learning neural networks is proposed as the solution to identify strange attractors in time-series multi-omics (scRNA-Seq) data and time lapse imaging of cancer stem cell differentiation. Cancer is discussed within the context of two unsolved foundational problems in science: the three-dimensional Navier-Stokes equations global regularity, smoothness and existence and the P vs. NP problem.

Preprints (www.preprints.org) | NOT PEER-REVIEWED | Posted: 27 June 2019 doi:10.20944/preprints201906.0288.v1

HYPOTHESIS: *A fluid-dynamics grid-scheme based Deep Learning neural networks is proposed as the solution to identify strange attractors in time-series scRNA-Seq data and time lapse imaging of cancer stem cell differentiation.*

PEDIATRICS: THE FUTURE

Cancer is the leading cause of 'disease'-related death among children in North America. According to the World Health Organization data, in 2015, near 397,000 children under 15 developed cancer globally and ~45% of those cases went undiagnosed (Oakes, 2019).

Leukemias, cancers of the bone marrow and blood account for ~30% of all pediatric cancers. Leukemia is myeloid or lymphocytic depending on which bone marrow cells the cancer originates. A leukemia is acute or chronic depending on whether most of the abnormal cells are immature (stem cell-like) or mature. respectively. Chronic myelogenous leukemia and Hodgkin's disease are now virtually curable. Acute lymphoblastic leukemia (ALL) is the most prevalent pediatric cancer. The uncontrolled proliferation of progenitor lymphocytes occurs usually by translocations/fusions. The 5-year survival rate for children has greatly increased over time, presently *>85%*. However, increased survival does not imply improved living conditions. Among children, B-cell lineage ALL constitutes approximately 88 % of cases while T-cell lineage represents the remainder. Multi-omics screening show epimutations shape CLL (chronic lymphocytic leukemia) lineages and can aid in clinical interventions (Gaiti et al.,2019).

Many relapse ALL has NT5C3 and CREBBP (CREB-binding protein) gene mutations (associated to chemoresistance). Poor prognosis for relapse (40%) occurs due to heterogeneity. >20% of patients show ETV6-RUNX1 mutation (best survival) and is the most common fusion gene in pediatric ALL while MLL-gene rearrangements occur in 6% (under 1 year of age). BCR-Abl1 and like subtypes, etc. are difficult to treat (Boer and Boer, 2017). Children whose leukemia cells have a translocation between chromosomes 12 and 21 are more likely to be cured with current treatments. Those with a translocation between chromosomes 9 and 22 (the Philadelphia chromosome) or 4 and 11 tend to have a less favorable prognosis.

Different subtypes are observed in young childhood (mostly ETV6-RUNX1 and hyperdiploid) whereas the frequencies are shifted in adolescent and young adults (from ~60 to 20%)—single cell CRISPR screens can identify many drug targets in these subtypes (Bhojwani et al., 2012). The time evolution of a cancer's molecular heterogeneity consists of hybrid (mixed) phenotypes, dormant states (quiescence) and the ability of one subtype to adaptively interconvert into another in relapse patients making it an intractable problem. For e.g. the whole genome sequencing of pediatric Wilms tumor, acute lymphoblastic leukemia (ALL) and acute myeloid leukemia (AML) identified sub-type specific clusters of driver events in many studies. There are fusion events and focal areas of gene deletion such as FLT3-ITD (FMS-like tyrosine kinase 3 -internal tandem duplication) with (wild-type 1) WT1 mutation or NUP98-NSD1 fusion with poor outcomes for AML. Children with leukemia cells that have translocations between chromosomes 15 and 17 (seen in most cases of Acute promyelocytic leukemia) or between 8 and 21, or with an inversion (rearrangement) of chromosome 16 have higher probability of being cured. Children lacking a copy of chromosome 5 or 7 (monosomy) or chromosome 5 deletion have poorer prognosis. Dysregulation of T cell mediated allorecognition is a driver of AML relapses post-hematopoietic cell transplantation (Health Statistics).

Preprints (www.preprints.org) | NOT PEER-REVIEWED | Posted: 27 June 2019 doi:10.20944/preprints201906.0288.v1

Hence, cancer is a dynamical, interconnected ecosystem with adaptive clonal heterogeneity. Even within a single patient, many adaptive subclones are found. Central nervous system cancers account for more than one-third of cancer death in children. Pilocytic astrocytoma and medulloblastoma are amidst the most common primary brain tumors in children between 5 -14 years of age and are the most common spinal cord tumors in the pediatric population. Although the 5-year survival rates are increasing, the quality of life is poor and children suffer from devastating side effects including secondary tumors/relapse in future, growth inhibition, disabilities, heart failure, kidney disease, infertility, etc. (Collins et al., 2015). With aggressive forms of brain cancer, barely 10 percent of children survive three years after diagnosis. Another deadly pediatric-killer is Glioblastoma Multiforme (GBM), malignant grade-IV tumors that are resistant to conventional therapies.

Exome sequencing of adult GBM identified 4 types of primary tumors: proneural, neural, classical and mesenchymal types. Aberrant gene expression of EGFR, NF1 and PDGFRA/IDH1 each define the Classical, Mesenchymal, and Proneural subtypes, respectively (Verhaak et al., 2010). The Proneural groups in the Verhaak classification consists of IDH (isocitrate dehydrogenase) mutants and can be low or high grade. The IDH1 mutants cluster of adult GBM favors mitochondrial oxidative phosphorylation. A more useful classification for gliomas in general is the 2016 WHO classification: IDH mutant vs IDH wild-type gliomas (Ceccarelli et al., 2016).

Response to aggressive therapy differs by subtype and patient, with the greatest relative benefit in the Classical subtype and no benefit in the Proneural subtype. However, all subgroups respond poorly to current treatments in neuro-oncology. Moreover, each patient's cancer is personalized, has unique molecular features that undergo clonal expansion and selection over time. It must be reiterated that within a single patient alone, the cancer is heterogeneous and adaptive. The genomic landscape of cancer in pediatrics is very different from that of adults (Sweet-Cordero and Biegel, 2019).The lower genetic mutational burden and higher epigenetic alterations in pediatric cancer has been postulated to be due to a combination of the embryonic origin of cancer, dysregulation of developmental pathways (morphogens) and environmental carcinogens. It is a highly complex ecosystem with single-cell molecular heterogeneity.

Mutations in IDH1 and less frequently in IDH2, occur in 80% of grade II and grade III astrocytomas and oligodendrogliomas, and are also found in high grade glioblastomas that have arisen over time from these lower grade gliomas (Staedtke et al., 2016; Azzarelli et al. 2018). In adults, the lack of IDH mutations, 1p19q co-deletion and/or presence of *BRAF* alterations are very helpful in sorting out the differential diagnosis. However, this does not apply in children, in whom *such mutations* are virtually absent. IDH1 mutants is only about 6% in pediatrics (mostly in adolescents, early adult-transition) (Ceccarelli et al., 2016). Thus, features of pediatric and adult cancers are very distinct.

IDH mutations disrupt cellular metabolism causing the hypermethylation of histones and CpG islands (methylator phenotype). Interestingly, progression to higher grade disease is often accompanied by overall decrease in methylation, but hypermethylation of a small subset of CpG islands associated with developmental regulators, including FOX, SOX and TBX family genes (which may arrest cells into a permanently self-renewing state) are observed (Bai et al., 2016). A common path of glioblastoma tumorigenesis is one or more of chromosome 7 gain, 9p loss, or 10 loss. TERT promoter/telomerase mutations often occurred later for rapid growth and relapsed tumors indicating a critical attractor in cancer development (Korber et al., 2019)

Preprints (www.preprints.org) | NOT PEER-REVIEWED | Posted: 27 June 2019 doi:10.20944/preprints201906.0288.v1

Survival promoting mutations commonly in TERT promoter is needed years pre-diagnosis of chromosomal alterations for detectable tumors. As well-established, the maintenance of telomeres (increased telomerase or ALT-alternative lengthening) is a hallmark of cancer. Recent studies showed 73% of cancers of 31 different types needed mutations in TERT promoter methylation (Barthel et al., 2017; Verhaak et al., 2019).

90% of GBM recurrences occur within 2 cm of original tumor resection site or radiation field. The post-operative residual tumor tend to be more aggressive post-non target specific therapies, especially if there is MGMT promoter methylation (confers chemoresistance) (Del Maestro, 2012). In 126 patients, those with more than 90% of tumour resection had a significantly better outcome, improving median survival from 225 to 519 days (Dea et al., 2012).

Surgical intervention of pediatric GBM sometimes may result in the rupture of the inner membranes attributing to the spreading of GBM (rare cases). GBM patients usually die within 15 months of diagnosis demonstrating their high aggressiveness and heterogeneity without metastatic invasion (Klughammer et al., 2018). The cancer lies very close to the blood-brain barrier and utilize GSC (glial stem cells), stromal cells and ECM (extracellular matrix-niche) through EMT (epithelial-mesenchymal transition) pathways to increase their cancer stemness, ATP/lactate production, tumor propagation and cancer-promoting signal transduction. Moreover, the inflammatory niche of brain cancers varies (e.g. DIPG shows a lower inflammatory milieu yet highly aggressive).

Epigenetic dysregulation is a hallmark of cancers especially in pediatric cancers, resulting in translocations and fusion oncoproteins accounting for some of the complexities in relapsed or refractory pediatric cases. Epimutations are more common in pediatric cancers than in adults (Filbin and Monje, 2019). The best-studied example of this is the histone-3 (H3)-K27M mutation that occurs in diffuse midline gliomas, such as diffuse intrinsic pontine glioma (DIPG) and thalamic and spinal cord gliomas of childhood (Filbin et al., 2018). For e.g. exome sequencing showed 7 hypermethylated samples in 19 patients, with TMZ (temozolomide) treatment+ angiogenesis inhibitor (e.g. bevacizumab) (Cancer Genome Atlas, 2008)**.** The most prominent difference between pediatric and adult cancers is the frequency of hotspot mutations in genes encoding histone H3 variants (0.2% in adults vs 50.3% in DIPG pediatric).

Epigenetic alterations often include complexes involved in chromatin remodelling such as SWI/SNF, polycomb repressor complexes and oncohistone mutations in GBM. Pediatric and young adult GBMs are molecularly distinct from adult GBM, with frequent alterations in H3.3-ATRX-DAXX (Salloum et al., 2017). For e.g. diffuse intrapontine gliomas have frequent histone gene H3F3A mutations. Whereas, CREBBP, SETD2 etc. play key roles in the altered epigenetic hallmarks of ALL. DNA methylation is highly aberrant in pediatric cancers especially brain tumors indicating a target for deep-learning studies (Det et al., 2018).

For instance, in Diffuse intrinsic pontine glioma (DIPG), the enzyme ACVR1 mutation cooperates with histone mutation H3.1 K27M in 20% of cases causing tumor development. K27M H3.3 tumours are found in 70% of DIPG and non-brainstem midline paediatric gliomas. The majority of DIPG patients carry a H3.3 Lys27Met (K27M) missense mutation, whereas a minority exhibit a H3.3 G34R/V mutation (Mackey et al., 2017). Hence, there are many partial patterns pertaining to epigenetic alterations that can be fed into artificial intelligence for the future of clinical care.

Preprints (www.preprints.org) | NOT PEER-REVIEWED | Posted: 27 June 2019 doi:10.20944/preprints201906.0288.v1

Treatment with immunotherapies such as PD-1 inhibitors (e.g. nivolumab or pembrolizumab) revealed a significant enrichment of PTEN mutations associated with immunosuppressive signatures in non-responders, and an enrichment of MAPK pathway alterations (PTPN11, BRAF) in responders (Zhao et al., 2019). However, there is low clinical efficiency of immune checkpoint inhibitors in GBM although nivolumab combo with ipilimumab is considered for recurrent GBM relapse. Most importantly, whether the most advanced of our current therapy regimes including immunotherapies target cancer exosomes is undetermined.

Functional genomics platforms and in vitro genome editing allows for efficient immunotherapies and multi-targeted CAR (Chimeric Antigen Receptor)- T cells. Arrayed CRISPR-Cas9 screens need to address immunomodulators, tumor microenvironments and in vivo effects of the cancer. Moreover, we must investigate whether arrayed CRISPR screens can be implemented on further aiding the proteomics assessments of the (heterogeneous) oncosomes from patients' liquid biopsies. Foundation Medicine is a commercially available platform for (selected) genomic profiling of tumors and includes screening of cancer immunotherapy biomarkers. Clinical commercial packages for nanoparticle medicine are also emerging such as Nanobiotix. However, a good commercial package for epigenetic sequencing and transcriptomics (multi-omics screening) is not clinically available (yet). Drug-Gene interaction databases (e.g. DGIdb) exist for finding genes in druggable categories although effectiveness is undetermined as seen in clinical trial outcomes.

CRISPR screens are effective tools to study chemoresistance in patients. CRISPR screens identified stemness regulators in patient-derived glioblastoma stem cells and sensitivity to chemotherapy including members of Sox (Sox9, Socs3, USP8, DOT1L and protein ufmylation) while TMZ-resistance genes were found to be Fanconi Anemia/ICL R, MCM8/MCM9, MLH1, mismatch repair genes, etc. (Macleod et al., 2019).

Conventionally, alkylated TMZ and radiation are usually administered for newly diagnosed GBM. Therapeutics targeting tumour angiogenesis concurrent with radiation is crucial to improve the overall therapeutic response in GBM (e.g. sunitinib, VEGF-inhibitors, glucocorticoids for edema-control, etc.) (Gerstner et al., 2009; Murayi and Chittiboina, 2016). However, with emerging complexities in cancer evolution, these approaches are not enough. For e.g. angiogenesis inhibitors are not effective against vasculogenic mimicry pathways.

GH (growth hormone) deficiency, neurological dysfunction and primary hypothyroidism are common after cranial irradiation and chemotherapy for nonpituitary-related brain tumors (Clarson and Del Maestro, 1999). Radiation and chemotherapy cause an acute depletion of (healthy) neural stem and progenitor cells. The long-term self-renewal capacity of neural precursor cells (NPCs) is diminished and NPC function is severely impaired by neurogenic - radiation-induced microglial inflammation. Moreover, these inflammatory pathways may increase the selection of more aggressive phenotypes in cancers.

Cancer is a systemic disease requiring multimodal therapies. Radio-oncology is often the route of treatment in aggressive stages of cancers. Radiation therapy releases ROS (reactive oxygen species)/free radicals and inflammatory responses, which not only can mutate healthy cells but can increase the survival of adaptive cancer stem cells. Abnormal scar tissues are generated by radiation therapy along with arterial venous malformations/shunts, arrested growth and sometimes secondary tumors. For instance, HIF-1 (hypoxia-inducible factors) signaling increases in chemo-resistant cells and ALDH1 (aldehyde dehydrogenase) increases radiation resistance. Note: proton therapy is less damaging than x-

Preprints (www.preprints.org) | NOT PEER-REVIEWED | Posted: 27 June 2019 doi:10.20944/preprints201906.0288.v1

rays when applicable. It must be investigated whether post-radiation oncosomes can horizontally transfer such adaptive traits as has been established for chemoresistance (Liauw et al., 2013). For instance, it is well-established NET (neutrophil extracellular traps) released from post-surgical stress and infections can induce cancer progression by collecting circulating tumor cells (CTC) and inducing the formation of metastases (Cools-Lartigue et al., 2013). Recent findings suggest non-target specific chemotherapy causes cancer cells to communicate about their microenvironmental changes by the release of pro-metastatic exosomes (Keklikogolu et al. (2019). Exosomes in the tumor microenvironment are hence mediators of cancer therapy resistance. Again, if such malignant traits are horizontally transferred through oncosomes in the case of radiation resistance must be investigated.

Childhood cancer therapies, such as cranial radiation, methotrexate and cyclophosphamide, induce persistent microglial reactivity which in turn induces neurotoxic astrocyte reactivity, disrupts oligodendroglial lineage dynamics, impairs myelination, blocks neuronal differentiation of hippocampal stem cells (neurogenesis) and contributes to aberrant pruning of synapses. Some of the current complications post-chemo/radiation therapies in neuro-oncology include: vascular- prothrombic neurological side effects, chemotoxicity, autoimmune responses, vasculitis, leukodystrophy, cognitive decline, delayed leukoencephalopathy with metabolic disorders, congenital issues, neuropathy, immunological inflammations, psychiatric symptoms, intravascular lymphomas, strokes, microangiopathy/cerebrovascular diseases, encephalitis, dystonia/dysmnesia, respiratory failures, secondary tumors/metastatic relapse, carcinomatosis, toxic metabolic encephalopathy, neoplasms/teratomas, etc**.** (Stewart et al., 1991). To overcome these health barriers, new ways of treating cancer must be devised and such is the attempt of cancer (stem cell) reprogramming.

Hence, mathematical models of cancer growth are critical to design optimal therapies for such adaptive systems. The "Go or Grow" hypothesis proposes that cell division and cell migration are temporally exclusive events and that tumor cells defer cell division to migrate. The oxygen shortage (hypoxia) in the environment of a growing tumour may well apply for GBM (Corcoran and del Maestro, 2003). Type IV collagen is a major protein component of the vascular basement membrane and its degradation by MMPs (matrix metalloproteinases) and enzymes is crucial to the initiation of tumor-associated angiogenesis and invasion. Group of tumor cells even amidst distant locations can release collagen IV degrading enzymes to the site of invasion, questioning the (non)locality of the cancer stem cell niche.

Childhood cerebellar tumors have conserved fetal transcriptional programs where cancer stem cells resemble embryonic stem cells (Vladoiu et al., 2019). Lineage-specific mechanisms that regulate stem cell behaviour in the embryo may be subverted in cancer causing its hyper-proliferation and differentiation. As known, stem cell niche pathways such as Wnt, Shh and Myc are embryonic developmental pathways in vertebrates. Sox2 (a Yamanaka factor) is also an essential driver of cancer stem cell sub-populations in glioblastoma (Suva et al., 2014; 2014) PI3K/mTOR (mammalian target of rapamycin) and MEK/ERK pathways were shown to be associated to the self-renewal in glioma stem cells (GSC) and mediate cancer stemness in brain tumors (Sunayama et al. 2010). For instance, in glioblastoma, induction of Gli1 by Nanog increases the clonogenic and tumorigenic potential of the CD133-positive stem cell fraction (Suva et al., 2013; 2014) The epigenetic landscape of GBMs (Glioblastoma Multiforme) shows tremendous spatiotemporal heterogeneity. However, a core set of neurodevelopmental transcription factors (POU3F2, SOX2, SALL2, OLIG2) were identified to be essential for GBM propagation in brain cancer stem cells (Suva et al.,2014). Thus, many GRN circuitries are being revealed with recent multi-omics mapping of pediatric cancers. Yet what distinguishes a cancer stem cell in a given tumor population’s evolution remains an unsolved problem, requiring the study of the fluid dynamics of cancer stem cell transitions and pattern formation.

Preprints (www.preprints.org) | NOT PEER-REVIEWED | Posted: 27 June 2019 doi:10.20944/preprints201906.0288.v1

As will be discussed, recent findings suggest simplified Navier-Stokes equations such as Darcy's law are required to better comprehend the reaction-diffusion processes underlying GBM invasion and growth. The tumor flow equations are proposed to help understand the complexity of gene regulatory networks (GRN) and thereby approach cancer stem cell reprogramming. In principle, a Waddington landscape can be reconstructed from any tumor sample from multi-omics data and the fluid flow equations can map the evolution of distinct phenotype clusters and its single-cell fate trajectories.

To summarize, quantitative changes of lineage specific Transcription Factors mediating cell fate decision-making can be revealed by single-cell RNA-seq and proteomics in early tumor progenitors (Taylor et al.,2019). A better understanding of the reaction-diffusion of morphogens pertaining to cancer stem cells and their energy landscapes is crucial to approach reprogramming cancer phenotypes. In principle, deep learning healthcare can analyze large datasets of pediatric cancer tissues, with single-cell molecular profiling of tumor biopsies and liquid biopsies (i.e. multiomics of exosomes, circulating tumor DNA, CTCs, etc.) to find optimal routes to reprogramming and in the meantime, provide Artificial Intelligence (AI)-assisted, personalized (precision) oncology.

On a final note, although cancer remains the primary 'disease'-related death in children, the 3 leading causes of injury-related deaths (accidents, excluding premature deaths) in North America in 2007 are motor vehicle accidents (MVA) (17%), drowning (15%) and suffocation (11%) (Yanchar et al., 2012). Accidents remain the primary cause of death of North American children. Childhood cancer contributes to less than 1% of all new cases in Canada. On a rather philosophical argument, what defines who are children; the age or the mental state? An estimated 1.2 million children and youth in Canada are affected by mental illness – yet, less than 20 percent will receive appropriate treatment (Health Canada, 2018). Of course, unmentioned are the horrors of human trafficking- a growing epidemic.

ENERGY LANDSCAPES

Waddington (1942) first described the cell developmental topography as an energy landscape where cell fate bifurcations are classically visualized as balls rolling up hills (energy barriers) and down valleys (attractors) (Bhattacharya et al., 2011; Wang et al., 2011). The cell fate decision making is governed by the gene expression dynamics of underlying regulatory networks. Due to the stochastic nature of molecules, the changes in molecular concentrations are generally defined by Langevin equations (Davila-Vederrain, 2015). The transitions between the attractors are considered as random walks on a network, following Boltzmann statistics (Perkins et al., 2014). The barrier heights and transition rates (epigenetic fluctuations) are in the order of thermal fluctuations k_BT, where k_B is the Boltzmann constant and T is the temperature.

As such, reactions are often modelled by Hills-Langmuir equations or Michaelis-Menten kinetics given their rates follow the Arhenius law: $Rate \propto e^{-\Delta G_a/k_BT}$ where G_a is the activation free-energy, and T the temperature. Noise in chemical fluctuations is often considered as a Gaussian term. However, this only holds for simple chemical reactions (i.e. central limit theorem) and biological reactions involve complex, nonlinear cascades with inhomogeneous energy potentials. Current models assume steady-state equilibrium for the reaction coordinates (Zhou et al., 2014). The dynamics of many biosystems are well described as random walks on a network: with three possible scenarios for the path distribution: finite, stretched exponential and power law (Perkins et al. 2014). The latter are used to describe the dynamics of the Lorenz attractor and G-protein folding. The Lorenz attractor is a strange attractor which gives the approximate description of a horizontal fluid layer heated from below. This is known as the Rayleigh-

Preprints (www.preprints.org) | NOT PEER-REVIEWED | Posted: 27 June 2019 doi:10.20944/preprints201906.0288.v1

Benard convection, a simple testable model of experimental fluid turbulence and used in weather forecasts (Lorenz, 1963).

Turbulent/chaotic chemical oscillations are neglected in Waddington landscapes since low Reynolds number (laminar) flows are assumed. However, turbulence can occur in very rapid bursts followed by laminar-like flows (intermittency). In complexity theory, these are NP-complete problems to which solutions of otherwise intractable problems can be verified by brute-force searching (i.e. stochastic methods). Gene expression is often naively considered a stochastic process (Elowitz, 2002).

An example of stochastic methods is evolutionary algorithms. Evolutionary algorithms are used to study the behaviours of collective dynamics like swarming and flocking of many-body systems in Artificial Intelligence. Consider the replicator equation with a free energy of the system given by:

$$F(q) = \sum_i q_i E_i - k_B T \sum_i q_i ln q_i = \langle E \rangle - TS(q)$$

The first term describes the energy of the state and the second term is the Shannon information entropy for a reaction coordinate q. At equilibrium, the Probability P of the system being in the i-th state is given by the Boltzmann factor and F is a measure of the fitness of the species (i.e. how it grows and spreads) assuming continuous Bayesian-hypothesis updating. Mutations help replicators evolve. The probability that a randomly chosen organism belongs to the i-th species is: $P_i = \frac{P_i}{\sum_j P_j}$. The fitness landscape well-defines current descriptions of the Waddington energy landscape.

The Langevin equation: $m\ddot{r} = F(r) - \gamma\dot{r} + \sigma\varphi(t)$ is used as the mass-equation of the Waddington landscape where the Fokker-Planck dynamics give the probability time evolution:

$$\frac{\partial \rho(r,t)}{\partial t} = \nabla \cdot (\nabla D - F\frac{1}{\gamma})\rho(r,t)$$

Where D is the diffusion coefficient, ρ the probability density, γ the friction/damping coefficient, F the force on the particle/molecule, r the relative polar coordinate, and $\sigma\varphi(t)$ is the fluctuation-dissipation term. In the Langevin equation, a particle undergoing a random walk has two forces- dissipative (proportional to velocity) and another of random character. Inertial force is neglected due to viscous drag assuming cells are highly viscous due to the macromolecule crowding, highly packed organelles and cytoskeletal filaments. Hence, the protein flows in tissue patterning (reaction-diffusion) are considered laminar as inertial forces are dominated by viscous dissipation (i.e. low velocity fluctuations). The Freidlin–Wentzell theorem gives the probability estimate of an Ito diffusion, a stochastic differential equation, as deviating from the mean trajectory on the landscape (Chunhe and Wang, 2013; Wang, 2015).

For an ensemble of cells undergoing bifurcations, the dynamics of a cloud (of cells) diffusing across the distribution of states on the attractor space is given by the Fokker-Planck equations

$$\frac{\partial \rho}{\partial t} = -\sum_i \frac{\partial}{\partial x_i}[A_i(x)\rho] + \frac{1}{2}\sum_{i.j} D_{ij}(x)\frac{\partial^2}{\partial x_i x_j}\rho$$

Preprints (www.preprints.org) | NOT PEER-REVIEWED | Posted: 27 June 2019 doi:10.20944/preprints201906.0288.v1

where the mean path is found from the Path integral formulation. D is the diffusion matrix, A is the drift vector, x the spatial coordinate and ρ the probability measure. The mean path is determined from an Onsager-Machlup functional (path integral) assuming a Gaussian kernel for the noise, as: $\rho(x,t) = \int Dx exp[-S(x)] = \int Dx \exp\{-\int L\big(x(t)\big)dt\}$ where the sum over all possible paths contributes to the trajectory. D is the diffusion coefficient matrix tensor, S is the action and L the Lagrangian or weight of each path. The conservation of probability flux is : $\frac{\partial \rho}{\partial t} + \nabla \cdot J = 0$ and the flux diffusion equation for the probability landscape is: $J = F\rho - D\nabla\rho$, which locally increases (source) or decreases (sink) the probability amplitudes. The fluctuation-dissipation driven cell fate commitments are often modeled using Hills equations and Gaussian noise terms (Wang et al. 2010; 2011)

A destabilization that results in the disappearance of an attractor state constitutes a bifurcation event in a nonlinear dynamical system. A single cell moves around an attractor basin over time, where the relaxation to a steady state potential is given by the Fokker-Planck equations (Li et al., 2016). However, certain marker/gene expressions can switch the cell fate from a basin of attraction into another, typically through chromatin remodelling (e.g. Yamanaka transcription factors). At the sudden critical shift of a system's configuration of steady states $x(t)$ (e.g. the nonexistence of the progenitor attractor), the effects of the bifurcation (control) parameter μ is given by, $\dot{x}(t) = F(x(t), \mu)$. In high-dimensional systems such as the Waddington landscape, the bifurcation parameters μ, are typically not known and used to denote qualitatively the critical transition state *(Mojtahedi et al., 2016). In fluid dynamics, the bifurcation parameter is often considered to be the Reynold's number (Ruelle, 1995).*

The energy potential at a given point in the landscape (i.e. a cell fate) is $V(x) = -\ln \rho(x)$. The potential V defines the attractor (energy minima) (note: this is assuming steady-state potentials, otherwise ρ(x, t) is complex to model as in the case of strange attractors). By convention, attractors (energy minima) in cell fate decision making are assumed to be fixed points or periodic orbits. However, in experiment, cell fates (even for non-cancer), fluctuate between attractors. Such fluctuations are characterized as stochastic processes (Huang and Kauffman, 2013). In argument, some of these attractors, especially in cancer ecosystems are proposed to be chaotic like the Lorenz attractor, where the cell fate can fluctuate back and forth between two valleys in an 'apparent random' motion. How to test the presence of Lorenz-like attractors in cancer/stem cell differentiation will be discussed in forth-coming sections.

Moreover, it remains a debated query whether Cancer stem cells are a small subset of a patient's cancer population (hierarchial model) or any tumor cell can revert its phenotype to stem cell state or if all cancer cells are potentially stem cells depending on its tumor microenvironment/niche? There is growing evidence to the latter, especially in aggressive pediatric brain cancers. Herein it is proposed, cancer cell fates are 'strange attractors' in the Waddington landscape. A strange attractor is a chaotic attractor with a fractal dimension.

Discrete Boolean networks show a probability distribution of states following a power law decay at transitions; a signature of scale-free, fractal organization (Font-Clos, 2018). The random walk on a network is assumed to follow the mean-square displacement law, where the anomaly parameter α decides if the particle trajectory is clustered or dispersed $\langle x^2 \rangle = Dt^{\alpha}$. Sometimes fractal filamentous structures emerge from diffusion-limited aggregation. For Boolean networks, spin glass topologies are used to model the 'fitness landscape' (e.g. the Kauffman NK model). The fitness landscape is the graph-theoretic representation of the energy landscape, that is the mapping of vertices of a finite graph to real numbers (e.g. gene expression values). In the NK model for instance, when a critical value of average number of connections to the nodes of a Boolean gene regulatory network are exceeded, the Hamming

Preprints (www.preprints.org) | NOT PEER-REVIEWED | Posted: 27 June 2019 doi:10.20944/preprints201906.0288.v1

distance between initially close two nodes grows exponentially in time (unstable regime) if there is chaotic attractors. The NK model is a tunable rugged energy landscape used in the computational modelling of the combinatorial optimization of GRN (gene regulatory networks) and complex systems (Kauffman and Levin, 1987; Weinberger, 1991). Hence, these are NP-complete optimization problems (i.e. can the optimum global minimum be computed amidst the local minima, for a nonlinear dynamical system?).

Spin glasses are tools to model complexity in a system of many-interacting agents and study how phase transitions occur in disordered states (emergence) (Mezard and Montanari, 2009). For e.g. EMT (epithelial-mesenchymal transition) states are reminiscent of glassy phase transitions. Lang et al. (2014), using single-cell gene expression data, demonstrated the Hopfield recurrent neural network (a spin glass) can reconstruct the corresponding cell states Waddington landscape. Taking the orthogonal projection of key transcription factors' gene expression creates a subspace defining an attractor. The energy minimization of the spin-glass Lyapunov function determines the landscape topography (Hopfield, 1982). Partially reprogrammed cell fates emerge as hybrids that co-express genes from multiple fates (spurious attractors) in the landscape (Lang et al., 2014).

The Gallavotti-Cohen fluctuation theorem is used to describe the phase space dynamics for ergostat dissipative systems (Evans and Searles, 2002). Yet the relative probability that entropy/information of a system far from equilibrium will increase or decrease in a given amount of time (i.e. the transition between two states) is given by $e^{-\Delta F/kT}$ where F is the free energy difference of the path integral. The Liouville/Moyal equation is used to describe the density matrix evolution if the quasi-probability distribution is modelled as a Wigner landscape (i.e. probability amplitudes can take negative values from a threshold).

Criticality in spin-glass phase transitions are reminiscent of chaotic bifurcations in pattern formation systems (Wolf et al., 2018). A reaction-diffusion model comprising of these complex bifurcations is the Fisher-KPP equation where the cell fate trajectories are depicted as branching diffusion trees and hence keep the random walk descriptions discussed above intact (Derrida and Spohn, 1988). According to this 'directed polymers on a tree' model, reaction-diffusion equations form travelling wave solutions. The speed of its wavefront is the free energy of the polymer and the minimal speed is the phase-transition into a glassy phase (Derrida and Spohn, 1988). The Cayley tree resembles the KPP-Fisher equation's trajectories while the free energy of the tree's wavefront is: $G(t) = \langle \exp(-\beta x)\, Z(t) \rangle$, where $\beta = \frac{1}{k_B T}$ and Z is the partition function. The wavefront velocity is dependent of its initial condition and accepts solutions of travelling waves given by $w(x - ut)$ where the velocity $u = \frac{1}{\beta} \log[k_B \int dV \rho(V) e^{-\beta_c V}]$ and V is the volume, if $\beta > \beta_c$. Here, β_c is the critical inverse temperature which is the effective noise parameter in Hopfield spin glasses as discussed by Lang et al. (2014).However, the probability density ρ (landscape topography) is assumed to be a Gaussian distribution, limiting the inhomogeneities and complexity of real energy landscapes. The result of these mathematics is a bifurcation tree with nodes at different points on the landscape (attractors) where the energies of the random walk change in time. At time t, there are $n(t)$ walks and $\langle n(t) \rangle = e^{\lambda t}$ where λ is the Lyapunov exponent or mean rate and t depends on diffusion D. Again, attractors can be of fixed points, limit cycles, periodic orbits or chaotic (i.e. strange attractors). The latter is proposed to be the solution to understanding cancer cell fates.

Preprints (www.preprints.org) | NOT PEER-REVIEWED | Posted: 27 June 2019 doi:10.20944/preprints201906.0288.v1

PATTERN FORMATION

Tumorigenesis is a subset of morphogenesis. Although the theory of reaction-diffusion is well-developed, the model depends on the 'system'. Single-cells exhibit molecular heterogeneity regardless of their pathological nature. However, cancer ecosystems exhibit complexity and far-from equilibrium pattern formation at every scale (i.e. gene expression, protein patterning and cell-ECM dynamics). Mathematical models of cancer generally revolve around *simplified Navier-Stokes equations* such as reaction-diffusion models, Darcy's law and predator-prey dynamics. How accurately do the current molecular models in vitro depict the complexity of cancers (even within the same patient) remain questioned.

Turing (1952) first coined the term morphogen to describe the chemical oscillations that result in coat patterns of animals. Stripes, spots and spirals self-organized from Turing's reaction-diffusion systems are given by nonlinear partial differential equations describing the dynamics of local morphogen concentrations. EMT-programs and related-proteins secreted by the CSC (cancer stem cell) niche remodel cancer phenotypes and the microenvironment through dynamic reciprocity. The general form of a 3D reaction-diffusion equation is given by:

$$\frac{\partial \boldsymbol{u}}{\partial \boldsymbol{t}} = \boldsymbol{D}\nabla^{\boldsymbol{2}}\boldsymbol{u} + \boldsymbol{R}(\boldsymbol{u}, \boldsymbol{t})$$

where u is the velocity vector (can be replaced by concentration c), ∇ is the gradient and R is the local reactions (coupling) term (note: this is Fick's second diffusion-law with a reaction term R). The simplest reaction-diffusion equation is the Fisher- Kolmogorov–Petrovsky–Piskunov equation (FKPP) (Fisher, 1937; Kolmogorov et al., 1937). A simplified growth-invasion system is given by the FKPP equations:

$$\frac{\partial \boldsymbol{N_1}}{\partial \boldsymbol{t}} = \boldsymbol{r_1 N_1}\left(\boldsymbol{1} - \frac{\boldsymbol{N_1}}{\boldsymbol{K_1}} - \frac{\boldsymbol{N_2}}{\boldsymbol{K_2}}\boldsymbol{\alpha_{12}}\right) - \boldsymbol{d_1 L_{N_1}} + \boldsymbol{\nabla \cdot (D_{N_1}(N_1, N_2)\nabla N_1)}$$

$$\frac{\partial \boldsymbol{N_2}}{\partial \boldsymbol{t}} = \boldsymbol{r_2 N_2}\left(\boldsymbol{1} - \frac{\boldsymbol{N_2}}{\boldsymbol{K_2}} - \frac{\boldsymbol{N_1}}{\boldsymbol{K_1}}\boldsymbol{\alpha_{21}}\right) - \boldsymbol{d_2 L_{N_2}} + \boldsymbol{\nabla \cdot (D_{N_2}(N_1, N_2)\nabla N_2)}$$

r_1 and $r_2$are the growth rates of normal and tumor tissue respectively, d the cellular susceptibility to excess acidic conditions, N_1 the normal tissue density, $N_2(r,t)$ density of the neoplastic and $L(r,t)$ the excess proton H^+ concentration (assumed normal tissue to be of logistic growth rate r_1 and carrying capacity K), α is the Lotka-Volterra (competition) strength, D is the respective diffusion coefficients and death rate is proportional to L (Gatenby and Gawlinki, 1996). For the neoplastic growth, it is the same equation denoted by a subscript 2 and a lack of death amidst excess acid (adaptive). Changes in oxygen and nutrient uptakes, especially in hypoxia (a signature of most glycolytic cancers), are modelled using such equations.

A two-species activator-inhibitor (A and B) model with their respective diffusion coefficients D, from the Turing (1952) model is given by:

$$\frac{\partial A}{\partial t} = f(A,B) + D_A\nabla^2 A$$

Preprints (www.preprints.org) | NOT PEER-REVIEWED | Posted: 27 June 2019 doi:10.20944/preprints201906.0288.v1

$$\frac{\partial B}{\partial t} = g(A,B) + D_B \nabla^2 B$$

assuming the intracellular protein oscillations have membrane and cytosolic bound state-transitions. Reaction-diffusion equations are used to model ECM (extracellular matrix) degradative enzyme dynamics, cytoskeletal proteins and adhesion modelling (Ramis-Conde et al., 2008; Domsuhke et al., 2014). In vitro models of cancer well-fit these equations where given chemoattractant gradients, degradative enzymes and nutrients concentrations, the ECM-stroma dynamics can be modelled as Turing reaction-diffusion (invasion) systems:

$$D = \nabla\big(-V(x,t)\big) + r\nabla A(x,t)$$

The first term is the direction of the potential V and the second is the chemotactic gradient of species A, where D is the diffusion coefficient. In a continuous description of tumor cell density, the number of cells N is given by the partial-differential equation $\frac{\partial N}{\partial t} = D_N \nabla^2 N - \nabla(N \nabla E)$ where E is the ECM density and $\frac{\partial E}{\partial t} = -\varphi ME$ and M the degradative enzyme. Considering additional equations for each enzyme rates and oxygen supply, glucose level, nutrients, etc., a simplified model of cancer morphogenesis is permitted. However, these models do not account for spatiotemporal chaos, tumor microenvironment-specific fluctuations and phenotype adaptiveness/plasticity of the complex ecosystem, to name a few absent parameters.

Variants of the Turing model are currently in practice in embryonic developmental biology. In the Clock and Wavefront model proposed by Cooke and Zeeman (1976), the morphogen wavefront progresses slowly in the anterior-to-posterior direction of a population of oscillators (cells) initiating EMT transition. Wolpert (1969) developed the French flag model where morphogens autonomously form segmented concentration gradients (Garric and Bakkers, 2018). Cells then respond to a specific level of morphogen gradient with a specific differentiation route by positional information of the molecules through the nonlinear feedback loops of Gene oscillatory networks (GRN) (Lauschke et al., 2013; Greene and Sharpe, 2015). Once again, chaotic oscillations/couplings of the oscillators are not accounted for in these models. After all, these are models for animal embryonic development and not necessarily cancer (stem) cells (i.e. model system-specific).

However ,signals involved in the vertebrate embryonic development such as FGF (fibroblast growth factor), Shh (hedgehog), VEGF (vascular endothelial growth factor), MMPs (matrix metalloproteinases), E-Cadherins, Wnt, TGF-β (transforming Growth factor), Notch/Nodal pathway, etc. are core embryonic stem cell niche pathways and EMT programs. The cancer-stem cell (CSC) niche exhibits aberrant expressions of these embryonic morphogens (Battle and Clevers, 2017).

Chaotic spatial heterogeneity (i.e. period-doubling bifurcations) can occur in a fluid, predator-prey system by coupling nonlinear chemical interactions to diffusion as seen in the Fisher-KPP equation (Pascaal et al., 1993). For instance, the Hagen Poiseuille flow (laminar flow in a cylindrical pipe) and FKPP equation $\frac{\partial c}{\partial t} = D\nabla^2 c + \rho c(1 - \frac{c}{c_{max}})$ have been used to model GBM growth, where c is the chemical species concentration and ρ is the tumor density (Cai et al., 2017, Altrock, 2015).

The Fisher-KPP equation was used as a prognostic indicator in breast cancer patients undergoing neoadjuvant therapy. The reaction-diffusion equations well-described tumor growth in accordance to clinical imaging data (Weis et al, 2015). The model well-characterized the reaction-diffusion based drug

Preprints (www.preprints.org) | NOT PEER-REVIEWED | Posted: 27 June 2019 doi:10.20944/preprints201906.0288.v1

delivery to tumors in clinical settings (Jarrett et al., 2018) The FKPP-model of GBM exhibits travelling wave solutions where the tumor invasion wavefronts have a velocity of $v = 2\sqrt{D\rho}$ (Harko and Mak, 2015). However, cancer in vivo, is surrounded by turbulent flows (i.e. turbulence at organ level can be >1000 and for exosomes in systemic flows, the Reynolds parameter should vary by a factor of 10^2- 10^3 as we transition from micro to nanoscale). Note: the flows are more crowded in lymphatic system than in circulatory system due to crowding by immune cells (neutrophils, macrophages, etc.), inflammatory proteins, ECM components, etc. (i.e. viscous flow).

Linear stability analysis of local equilibria and Darcy's law can model GBM patterning (Yan et al., 2017). Turing equations were shown to well-describe cancer-immune cell invasion dynamics (Zheng et al., 2018). Another recent GBM model is given by Darcy's law where the mass-averaged velocity of solid components u_s is defined as:

$$u_s = -(\nabla P - \frac{\delta E}{\delta \varphi_T} \nabla \varphi_T)$$

Where $\varphi_T = total\ tumor\ volume$, E the adhesion energy given a double-well potential and P is the solid pressure (Yan et al., 2017). Darcy's law can be derived from the 3D Navier-Stokes equations for a shallow flow between two plates.

Recently, a simulation modeled skin to behave like a 2D fluid where viscous forces determines pattern formation. Hydrodynamic interactions created patchy, isolated islands of cancerous patterns (melanomas) (Hoshino et al., 2019). Patchiness is a signature of turbulent flows (intermittency).
The lateral inhibition in embryonic pattern formation has been described as optical phonons (quantized vibrations) on a lattice, hence, new physics are emerging in the description of morphogenesis (Negrete et al., 2019).

Chaos in physiological systems is well-established. An intensively studied system is the Mackey-Glass equation, a first-order nonlinear, time-delay differential equation used in many physiological feedback systems, especially hematopoietic control/diseases (e.g. leukemia). As the time-delay increase in the release of circulating WBC (white blood cells), state-dependent (chaotic) period-doubling bifurcations emerge as in the case of leukemia patients (Mackey and Glass, 1977). However, the time-delay dynamics of exosome release by cancer patients is not established and is crucial to approach cancer complexity.

The Rössler attractor is an example of a strange attractor observed in simple chemical reaction-diffusions (Rössler, 1976). The Sel'kov model for glycolysis is an important metabolic pathway in which glucose is broken down to make pyruvate. The model exhibits a Hopf bifurcation in glycolytic oscillations (Rensing and Jaeger, 1985). Chaotic oscillations of a single transcription factor can be used to up-regulate certain proteins, or specific protein complexes (Heltberg et al., 2019).

Chaotic cancer attractors emerge in the reaction-diffusion modelling of tumour growth depending on changes in the control parameters (i.e. oxygen concentration, glucose level, tumor volume, diffusion from surface and growth- parameters) (Itik and Banks, 2010). Lyapunov exponents and fractal dimension were calculated for cancer patterning. While the Lorenz attractor has a fractal dimension of 2.06, the cancer models showed ~2.03 indicating a chaotic attractor with Shilnikov-bifrucations (Itik and Banks, 2010).

Preprints (www.preprints.org) | NOT PEER-REVIEWED | Posted: 27 June 2019 doi:10.20944/preprints201906.0288.v1

Ivancevic et al. (2008) show a Lorenz-like, chaotic attractor best describes the reaction-diffusion of cancer given by $\frac{\partial \varphi}{\partial t} = \nabla \cdot (D(\varphi, v)\nabla\varphi(v, t))$ where φ is the density of diffusing material (cancer cells). The emergence of Lorenz-like attractors indicates cancer cell fates are strange-attractors of the Waddington landscape. As opposed to being fixed in a single valley (attractor), a cell fate fluctuates back and forth between two or more valleys in an unpredictable behaviour.

The Navier-Stokes equations for an isotropic, incompressible Newtonian flow (i.e. $\nabla \cdot u = 0$) is given by:

$$\frac{\partial \boldsymbol{u}}{\partial \boldsymbol{t}} = \boldsymbol{v}\nabla^2\boldsymbol{u} - \boldsymbol{u} \cdot \nabla\boldsymbol{u} - \frac{\nabla \boldsymbol{P}}{\boldsymbol{\rho}} + \boldsymbol{f}$$

Where u is the velocity vector, v the kinematic viscosity, P is the pressure, ρ the fluid density and f is the external forces. The nonlinear partial differential equation was reduced to a 1st order-coupled ODE (ordinary differential equation) to form the Lorenz attractor (Lorenz, 1963). Interestingly, a variant of FKPP describes Rayleigh-Bernard convections when the reaction term R(u) = u (1 – u^2) (Newell and Whitehead, 1969).

Electric cell impedance recordings were performed in rat's prostate cancers. The time-series, Fourier analysis of cancer micro-motions were assessed by Taken's theorem to detect patterns distinguishable from a random signal. That is, the time-series data was embedded at least 2N+1 dimensions given N data dimensionality with a fixed time-lag. The attractor reconstruction showed positive Lyapunov exponents in phase portraits (i.e. signature of chaos) (Posadas et al., 1996). Time-delay Hopf bifurcations can indicate tumor relapse indicating aggressive stages of cancer (indicative of increased chaotic behaviour) (Khajanchi et al., 2018). Through time-series cancer data (i.e. time lapse imaging of intracellular proteins' reaction-diffusion and time-series multi-omics data), signal processing methods such as wavelet analysis, object edge detection algorithms, velocimetry profiling and spatiotemporal intensity-correlation analysis (STICS) to name a few, lag-time embedding can compute phase portraits of chaotic attractors. The time lapse imaging of reporter-intracellular proteins in pattern formation (e.g. reaction-diffusion of PAR cell polarity complexes, EMT pathways, cancer stem cell niche factors, etc.) and time-series data of stem cell differentiation in cancer are ideal data sets to identify *strange attractors* (Briane et al., 2018).

Cancer modelling was performed using a three-body ecosystem consisting of host, immune and tumor cells. Assuming initially logistic growth, the Lotka-Volterra dynamics became chaotic as denoted by the Feigenbaum period doubling cascades in the bifurcation diagrams (Letellier et al., 2013). The bifurcation analysis revealed Rossler-like attractors with a fractal Lyapunov dimension. Letellier et al. (2013) further propose the understanding of tumor growth and metastasis as strange attractors will pave 'dynamical therapies' (i.e. how drugs alter the fractal complexity and chaotic structures of cancer?).

Therefore, fractal dimension algorithms such as box-counting, correlation analysis, Fourier spectrum, etc. and phase portraits/Lyapunov spectra are tools that must be implemented on time-lapse imaging of cancer (stem) cell differentiation/division with specific protein reporters to identify strange attractors. Strange attractors can be identified with their continuous power spectra/ frequency analysis. Attractor reconstruction methods must be repeated for chemical oscillations of other proteins that are critical for cancer pattern formation. For e.g. Do strange attractors emerge in the time-series imaging of PAR complexes distribution in cancer cell division?

Preprints (www.preprints.org) | NOT PEER-REVIEWED | Posted: 27 June 2019 doi:10.20944/preprints201906.0288.v1

Strange attractors are bounded regions of phase space with positive Lyapunov characteristic exponents and a fractal dimension. Strange attractors are signatures of the frequency-spectra of turbulent hydrodynamics (Ruelle, 1995). Cancer is a multiscale, systemic problem. The use of reaction-diffusion systems to predict cancer dynamics has been compared to forecasting weather patterns using fluid dynamics equations (Yankeelov et al., 2013; 2015; Tang et al., 2014). An unresolved multi-scale flow problem is that of *turbulence*.

REPROGRAMMING

Reprogramming cell fates was an intractable problem until the pioneering works of 2012 Nobel Laureates Shinya Yamanaka and John Gurdon. Today, the Yamanaka factors can be replaced by a cocktail of small molecules. For e.g. Forskolin, 2-Me-5HT and D4476 to substitute for Oct4 and VC6T (combination of VPA (valproic acid), CHIR99021 (GSK3-inhibitor/Wnt activator), 616452 (TGF-β RI Kinase Inhibitor II) and Tranylcypromine) can reprogram mouse embryonic fibroblasts to iPSC (induced pluripotent stem cell) states (Hou et al., 2013). For e.g. Dppa2/3 facilitates the epigenetic remodelling during reprogramming to pluripotency, an overexpression of which increases reprogramming of fibroblasts to iPSC from 1-2% efficiency to near 80%. It targets chromatin decompactification via DNA damage responses and associated histone marks (γH2Ax) (Hernandez et al. 2018). The chromatin remodelling allows the facilitated binding of Yamanaka TFs and overcome the epigenetic barriers to dedifferentiate cells to iPSC states. Of all reprogramming techniques, the early retroviral induction presents the lowest efficiency. miRNA-367/302 and synthetic mRNA encoding reprogramming factors generated iPSC clones claimed with up to 90% efficiency in human fibroblasts (Kogut et al., 2018). High efficient miRNA reprogramming methods such as miR302, increases Oct 4 gene expression and suppresses HDAC2 (histone deacetylase 2). Many alternate algorithms have been discovered for altering the epigenetic energy landscape and minimizing the trajectories towards pluripotency attractors (Rais et al., 2013).

Current efforts are aimed towards reprogramming somatic cells to totipotency (Barker and Pera, 2018; Etoc and Brivanlou 2019). Retrovirus reprogramming to embryonic stem cells can induce a small subset of 2C-like states (2-cell) which fluctuate in cell fate, partially due to histone-modifying enzymes (Macarlan et al., 2012). Chemical reprogramming platforms and single cell RNA-sequencing allows reconstructing the progression trajectories and cell fate dynamics of stem cells. Hi C Seq and time-series scRNA Seq are used to determine GRNs of cellular reprogramming networks and thereby can pave cancer stem cell reprogramming (Ranquist et al., 2017; Zhao et al., 2018). Time-series scRNA-Seq and multi-omics will allow us to map cancer stem cells as dynamical systems, whereas most of our current approaches are static. In proposition, the reprogramming of cancer stem cells relies on identifying the nodes of GRN that causes chaotic cell fate transitions and turbulent pattern formations (i.e. strange attractors). Moreover, current findings suggest CSC (cancer stem cell) developmental plasticity and their phenotypic characteristics are less constrained than believed (environment-dependent), highlighting the higher epigenetic burden of pediatric cancers (however, highly debated).

Stem cell fate transitions encounter many fluctuations and molecular heterogeneities. For instance, Nanog heterogeneity arises from fluctuations in gene networks and sudden burst-like transcription (intermittency) in the coexisting states (Smith et al., 2017). LIF (leukemia-inhibitory factor) and 2i (2 small molecule inhibitors; GSK3β inhibitor/Wnt activator and MEKi (blocks MAPK pathway)) with TGFβ (transforming growth factor beta) signaling modulation can keep mouse Embryonic stem cells in a

Preprints (www.preprints.org) | NOT PEER-REVIEWED | Posted: 27 June 2019 doi:10.20944/preprints201906.0288.v1

pluripotent state by upregulating the triad of Nanog/Oct4/Sox2 (similar algorithm for humans). For instance, a similar chemical cocktail of small molecules were shown capable of reprogramming human fetal astrocytes into neurons (i.e. change cell lineages) (Yin et al., 2019). It remains a query whether chemical conversion algorithms exist for reverting cancer phenotypes and is the purpose of this communication. However, in the context of cancer stem cells, signals effects vary on tissue type and microenvironment (O'Brien-Ball and Biddle, 2017). For e.g. TGFβ is oncogenic in some settings and tumor suppressive in others (Haigis et al., 2019). Cancer stem cell fates are chaotic dynamical systems and thereby highly unpredictable, partially owing to complexities such as quiescence/dormancy and long-lived partially reprogrammed states (hybrids, EMT-MET) and identifying these states remains an intractable problem due to their dynamic, environment-dependent complexity.

The primary strategy used for inducing CSCs (cancer stem cells) is to enrich the cells using classical stem cell markers (clusters of differentiation) such as CD13, CD24, CD44, CD47, CD90 and CD133, followed by other techniques including side-population analysis, CyTOF cytometry and sphere formation. They are examined further according to their cancer markers such as WNT, Notch, Hedgehog, TGF β, epithelial–mesenchymal transition (EMT) signaling proteins, Yamanaka factors and epigenetic factors/histone modifications. Note: The Myc network, one of the Yamanka factors, may be a common point between cancer and embryonic stem cells and a key target for exosome-dependent cancer phenotype reprogramming (Kim et al., 2010; Yan et al., 2018).

Transcriptomics revealed glial-tumor interactions in tumor microenvironment form neuroinflammatory signals regulating brain metastases such as upregulated EMT/MET pathways and calcium signaling (Wingrove et al., 2019). The identity of CSCs to drive tumor growth and resistance have been challenged in brain tumors. A recent finding shows cells expressing CSC-associated cell membrane markers in Glioblastoma (GBM) do not represent a clonal entity defined by distinct functional properties and transcriptomic profiles, but rather a 'plastic state' that most cancer cells can adopt (i.e. phenotypic heterogeneity arises from non-hierarchical manner) (Dirkse et al., 2019). Unlike the glycolytic cancers (Warburg effect), GBM rely mostly on fatty acid oxidation for proliferation (Duman et al., 2019). In argument, cancer stem cells are plastic states with reversible fate transitions instructed by the microenvironment. If such is true, cancer cell fates are reprogrammable (Dirkse et al., 2019). Glioma cells in a subset of mesenchymal tumors were shown capable of losing their neural lineage identity, express inflammatory genes, and co-exist with marked myeloid infiltration, reminiscent of molecular interactions between glioma and immune cells. t-SNE projections of scRNA-Seq in GBM found cellular subpopulations resembling different expression subtypes co-occurring in the same tumor that adapt heterogeneous phenotypes in disease progression (Patel et al., 2014; Yuan et al., 2018) Hence, all GBM cancer cells are claimed to be cancer stem cells as opposed to hierarchy-based clonal subsections.

On the other hand, another paper's findings suggest conserved neural trilineage cancer hierarchy with glial progenitor-like cells at the apex (Couturier et al., 2018) A droplet based scRNA Seq- of cells from a given patient, generated two or three cancer groupings by t-distributed stochastic neighbour embedding (tSNE) and the Louvain community detection algorithm, clustering different clones within a tumour. Following PCA (principal component analyses) to assess intratumoral heterogeneity in the enriched GSCs of each group, the data suggest that GSCs are organized into progenitor, neuronal, and astrocytic gene expression programs, resembling a developing brain. Strong correlations were found in pathways such as EZH2, FOXM1, and Wnt, as relevant to cancer stem cell self-renewal and tumorigenicity. Targeting E2F blockers were shown to preferentially affect progenitor GSC proliferation in xenografted mice (Couturier et al., 2018). However, the paper does not reject the micro-environment dependent phenotypic plasticity and interconvertibility of cell fates. Hence, whether there is a fixed hierarchial

Preprints (www.preprints.org) | NOT PEER-REVIEWED | Posted: 27 June 2019 doi:10.20944/preprints201906.0288.v1

clustering or any cancer cell can acquire (or is in) a stem cell fate depending on its environmental cues, is a highly debated, unsolved problem. Again, these findings are not necessarily contradictory. Cancer being a dynamical system, these data sets must screen time-series scRNA-Seq of cancers in different microenvironmental contexts.

A core set of neurodevelopmental transcription factors (POU3F2, SOX2, SALL2, OLIG2) were identified to be essential for GBM propagation in brain cancer stem cells (Suva et al., 2013; 2014) GBM stem cells produce heterogeneity through wound healing pathways and EMT programs to migrate. These pathways are used to reprogram human skin fibroblasts to tumor-infiltrating cytotoxic stem cells for therapy (Bago et al., 2017) Note: stem cells plasticity on glass/in vitro and in vivo are highly different. Moreover, tumor initiating cells have elevated methionine cycles. Hence, the high consumption of exogenous methionine (a precursor of methylation state of cancer cells) may be a newly emerging hallmark of cancer (Wang et al., 2019). CSCs with the ability to form secondary tumours have been shown to downregulate natural killer (NK) cell activator molecules when they transform into a quiescent state, through a mechanism involving autocrine inhibition of Wnt/β-catenin signalling by DKK1 (Malladi et al., 2016). These are merely examples to illustrate the dynamical complexity of cancer ecosystems and why reprogramming cancer cell fates remains an intractable problem.

The first-discovered, clinically relevant tumor biomarker is CEA (carcinoembryonic antigen). It is highly elevated in certain fetal tissues and found elevated in ~70% cancer patients' blood tests (Gold and Freedman, 1965). Since then, the search for universal tumor biomarkers has now tuned into liquid biopsy targets: ctDNA (circulating tumor DNA), CTC (circulating tumor cells), exosomes and their and associated epigenetic signatures.

Exosomes are usually 30-100 nm sized, heterogeneous packets of information released by cells forming cell-cell and cell-matrix communication networks. Tumor extracellular vesicles (EVs) mediate the communication between tumor and stromal cells, travel to distant regions from bloodstream or lymph vessels and form the pre-metastatic niche to promote metastases (Guo et al., 2019). Exosomes horizontally transfer therapy resistance to tumor cells and induce their aggressive development (Wei-xian et al., 2014; Hu et al., 2015; Zhang et al., 2018). It remains a query whether oncosomes exhibit nonlocal effects due to their nanoscale.

Current EV characterization typically consists of three factors: the nanometer size exclusion (sometimes density), shape under transmission electron microscopy (cup shape) and surface markers (e.g. TSG101, CD9, CD36, CD81, etc.). The technique of isolation affects the results as well (for e.g. impurities such as lipoproteins, immunoglobulins, immune factors form in ultra-centrifugation). Dynamic light scattering and nanoparticle tracking devices are used for exosome detection by studying its Brownian motion as well.

Proteins are usually identified by LC/MS-MS (mass spectrometry) in EVs from patient's blood plasma and hence serve as diagnostic indicators for early detection. Other proteomics/ sequencing methods exist for studying exosome cargoes. Exosomes can be used to monitor disease progression due to their unique cargo/biomarkers such as microRNA, nucleic acids, and pool of proteins found in the EVs. Exosomes are especially useful in relapse patients (prognostic indicators) to derive targeted therapies for the aggressive stages. The biomarkers change in type and concentration as the cancer evolves indicating the adaptive changes in the tumor microenvironment (Lane et al., 2018; Huang and Deng, 2019). Tumor biomarkers from liquid biopsies consist of circulating miRNA, ctDNA/cell free tumor DNA,

Preprints (www.preprints.org) | NOT PEER-REVIEWED | Posted: 27 June 2019 doi:10.20944/preprints201906.0288.v1

circulating tumor cells and EV bodies of tumor derived exosomes (also their post-translational modifications, e.g. methylation pattern of ctDNA). For e.g. normal exosomes may contain abundant actin and ribosomal proteins, whereas oncosomes express higher levels of oncoproteins like p53, Her-2, etc. (specific to cancer and stage) angiogenic factors (VEGF, Hif-1), etc. The nucleic acids inside exosomes can be sequenced (e.g. methyl-C-Seq, RNA-Seq), proteomics analyses can be assessed on the vesicle cargo and surface markers expressions can be assessed by flow cytometry. Surface markers vary by cancer, patient, and the dynamical tumor microenvironment (time). With relapse, the cargos are more specific to the patient and reminiscent of the recurrent tumor phenotypes. For instance, the EVs in relapse or stage III melanoma were enriched with mutant BRAFv600E in the lymphatic exudate (Garcia-Silva et al., 2019).

Nanoflow cytometry shows EV output of glioma cells are highly heterogeneous. For instance, EVs released by EGFRvIII-transformed cells were enriched for extracellular exosomes and focal adhesion related proteins. There was a high association of pro-invasive proteins (CD44, BSG, CD151), while the EGFR negative cells released CD81 expressing EVs. Regardless of the markers, the EVs of EGFRvIII expressing glioma cells caused the GBM to spread (Figueroa et al., 2017; Choi et al., 2018). These EVs are detected in the patient's cerebrospinal fluid. Hence, exosomes are heterogenous and adaptive, indicating alternative biophysical and complexity-based (machine learning) approaches are required for exosome screening/profiling. Moreover, the EGFR/PI3K/Akt pathway is a critical feedback loop allowing fatty acid metabolism and lipid synthesis in the survival of malignant gliomas (Guo et al., 2013). The adaptive heterogeneity in GBM post-conventional therapies is its signature. Post-surgical stress can induce inflammatory responses activating the cancer stem cell niche (e.g. cancer associated fibroblasts, chemokines/cytokines, NETs (neutrophil extracellular traps), etc.) and thereby induce GBM invasion and metastases. Post-therapy, the environment can transform the previous cell clusters into newer aggressive GBM phenotypes (e.g. some glioma will transform into gliosarcoma, another malignant cancer). Another complexity in most refractory cancers is senescence and transitory states from dormancy (edge of chaos).

For e.g. pancreatic ductal adenocarcinoma (PDAC) is a highly lethal disease characterized by late diagnosis, adaptive heterogeneity and treatment resistance. Various Moffitt transcriptomic subtypes have been identified using Imaging mass cytometry and molecular profiling/RNA Seq (for e.g. GATA 6 (activates Wnt pathway) is high in the classical subtype of pancreatic cancer) (Martinelli et al., 2017). The presence of hybrids or reversible mixed types in relapse are still in query. However, senescence is a crucial factor behind its intermittency and relapses. Pancreatic cancers are usually highly hypoxic and activate cancer associated fibroblasts (CAFs) to secrete extracellular matrices that confer its protective and hypoxic cancer stem cell niche. The ECM-niche (tumor microenvironment) signaling is what determines cancer cell fates and hence can convert a transitory state or growing cancer cell into a cancer stem cell (and vice versa). For instance, the pancreatic stellate cells produce vitamin A and vitamin C. In cancer, these convert into cancer associated fibroblasts (CAFs) and fuel cancer stemness. Hence, the supply of retinoic acid and calcium/vitamin D inducing drugs are used to revert these states.

Regardless of the cellular complexity, the pancreatic cancer exosomes are governing the pre-metastatic niche dynamics (Costa-Silva et al., 2015).CXCR2 inhibitors used in asthma/respiratory illnesses can disrupt tumor-stromal interactions in pancreatic cancers and inhibit NETs (neutrophil extracellular traps) transmissions from tumors (Dart, 2016). Verapamil for instance, a calcium channel blocker and anti-hypertensive, is effective in treating some pancreatic cancers. The molecular heterogeneity of such

Preprints (www.preprints.org) | NOT PEER-REVIEWED | Posted: 27 June 2019 doi:10.20944/preprints201906.0288.v1

complex adaptive ecosystems suggest personalized pharmacogenomics is the current optimal approach to oncology until the discussed reprogramming methods are proven otherwise (Zhao et al., 2016).

The In vivo tracking of exosomes with multiplexed EV Reporters and intravital microscopy or bioluminescence imaging is another emerging clinical tool for early detection of cancer/relapses. For e.g. luciferase/Rluc or Gluc (biotin acceptor protein) combined with transmembrane domains, such as lactadherin, label exosomes and are coupled with medical imaging-based techniques for tracking the spatiotemporal distribution of EVs in vivo (Chao et al., 2018) For e.g. EV-GlucB were injected into athymic nude mice via the retro-orbital vein and live imaged. The tetraspanin marker and CD63-pHluorin (pH sensitive GFP derivative) with luciferase-biotinylation were used as exosome tagging methods with total internal reflection fluorescence and dynamic correlative light–electron microscopy for in vivo tracking (Verweij et al., 2018; Lai et al., 2014; 2015). Moreover, exosomes are promising drug delivery technologies as well (Gangadaran et al., 2018; Chao et al., 2018))

Clinically, exosomes derived from serum samples of patients with glioblastoma bear specific EGFR VIII (epidermal growth factor receptor 8), reinforcing tumor-derived exosomes as sources of biomarkers reflecting the status of origin cancer cells (Skog et al., 2008) Exosomes are being recognized as diagnostic tools in other diseases too. For instance, neurofilaments and amyloid fibril proteins are found abundantly in Alzheimer's patient exosomes (Sinha et al., 2018). While the search for biochemical signatures across cancer exosomes is a current problem, there should be greater emphasis on the biophysical properties of oncosomes such as their flow visualization, vibrational properties, spectroscopic (frequency) analyses, etc. Moreover, non-target specific chemotherapy is known to cause cancer cells to release pro-metastatic exosomes (Keklikogolu et al., 2019). Hence, targeting exosomes should be the direction of future therapies in oncology.

However, the most prominent feature of exosomes is as reprogramming machineries of cancer phenotypes. The human embryonic environment can suppress cancer phenotypes, via extracellular vesicles (Camussi et al., 2011; Zhou et al., 2017). An embryonic microenvironment might have the capacity to reverse the metastatic phenotype of cancer cells where exosomes from hESC (human embryonic stem cell) microenvironment has recently been shown to reprogram malignant phenotypes to healthy-like plastic states (Zhou et al., 2017). The reverse also holds true (i.e. Horizontal transfer of malignant traits via oncosomes to healthy phenotypes) (Abdouh et al., 2017). An elevated expression of the Yamanaka factors in the vesicles were shown crucial for the plasticity transformation. Exosomes can reprogram distant cells/tissues and transform the microenvironment towards oncogenic tumor microenvironments serving as hotspots for metastases.

The understanding of the cooperation between tumor-derived exosomes and NETs in cancer-associated thrombosis is emerging. Nanoparticle tracking analysis and imaging microscopy show tumor stem cell-derived oncosomes prime neutrophils and NETs to promote cancer progression by developing the inflammatory conditions for a pre-metastatic niche (Leal et al., 2017; Hwang et al., 2019).

Multi-omics can map embryonic stem cells bifurcating to pluripotent states, where the phosphoproteome dynamics (kinase-substrate networks) precede the changes in epigenome and transcriptome governing cell fate transitions. The signaling dynamics of ERK, mTOR (mammalian target of rapamycin), etc. were shown to be critical in such early state bifurcations (Yang et al., 2019). Recent clinical trials show RNA-Seq and proteomic assessments increase the molecular targets in precision oncology (Le Toumeau et al., 2019; Rodon et al., 2019). The TARGET study shows analysis of ctDNA

Preprints (www.preprints.org) | NOT PEER-REVIEWED | Posted: 27 June 2019 doi:10.20944/preprints201906.0288.v1

mutations matching with tumor biopsy provides more precise molecular targets in patient-care. Other research-platform based tools are emerging that may help clinical oncology as well. For instance, screen drug sensitivity assays for in vivo xenografted organoids has been demonstrated in ovarian cancers (Kopper et al., 2019) Organoids, CRISPR screens and most importantly multi-omics screening/scRNA-Seq analysis will provide precision oncology. The molecular profiling of patients' tumor/liquid biopsies, microbiota, inflammatory markers, etc. can be fed into deep learning algorithms for optimal clinical decision making (e.g. IBM Watson).

A biomarker does not have to be an expressed molecule, driver mutations, methylome patterns in ctDNA, etc. It can be a characteristic pattern in the frequency spectra, a vibrational signature (e.g. Raman spectral band) or flow patterns (reaction-diffusion kymograms) in time-lapse imaging. Hence, even an equation that distinguishes normal phenotypes from the pathophysiology of interest is a biomarker (i.e. a strange attractor/ NSE equations as proposed for cancer). Hence, the biophysical properties of exosomes such as their flow patterns and spectroscopy bands (e.g. vibrational spectra) are emerging cancer biomarkers.

ARTIFICIAL INTELLIGENCE

Complexity theory is the study of complex systems, their emergence, self-organization, nonlinear dynamics and the multiscale modelling of their interaction networks. Biocomplexity provides a holistic, systems biology approach (i.e. the whole is greater than the sum of the parts) to cancer ecosystems with interdisciplinary techniques. Complexity is related to NP completeness, as seen with decision-making and optimization problems in cancer ecosystems. Cancer, however, is a complex adaptive system. That is, the interacting parts respond to the stimuli of the environment and changes its behaviours through feedback loops (signal transduction). The Hanahan-Weinberg hallmarks (e.g. autocrine feedback/self-regulated growth signals, telomerase overexpression, immune evasion/invasion, anti-apoptosis/death, etc.) highlight cancer adaptiveness.

Question: Is searching necessary to find a needle in a haystack? This depends on our tools, if we had a magnet, we don't have to explore the vast space of possibilities to find the needle. This is an analogy of optimization. Finding the clique/master GRN (gene regulatory networks) controlling CSC cell fate transitions or modelling protein folding for instance are such searching problems that are combinatorially complex. The P vs. NP problem asks, can we solve searching problems without searching? NP (non-polynomial) problems are quickly checkable but solved by searching (difficult). Are easily checkable problems also easily solvable is the question. The problem was first informally addressed in a letter by Gödel to von Neumann (1956). If P=NP, then if you solve one problem, you solve a class of similar problems. The NSE is a complexity problem whereby the search for strange attractors is the algorithm (magnet).

Phase transition (percolation) is when a few connections of a sparsely connected digraph system flips to a rich connectivity or vice versa (i.e. a network fragmented into small clusters) as in the transition from laminar to turbulent flows (Lemoult et al., 2016). Phase transitions describe illness onset and immune network breakdowns (edge of chaos) (Bossamaier and Green, 2000). To identify a minimum number of transcription factors to reprogram cell states to pluripotency was an NP-problem, experimentally solved by Yamanaka, Gordon, et al. The query now lies on whether cell states can be reprogrammed to earlier fates or more importantly reprogramming in a disease context (i.e. cancer stem cells to non-malignancy). Cancer phenotype is reprogrammable to non-malignancy by its environment, as has been demonstrated by the transfer of exosomes from sera (Zhou et al., 2017). However, identifying the

Preprints (www.preprints.org) | NOT PEER-REVIEWED | Posted: 27 June 2019 doi:10.20944/preprints201906.0288.v1

minimal circuit to reprogram cancer cell states is currently a complexity problem. The solution is herein proposed to be strange attractors in the cancer GRN (i.e. not necessarily transcription factors but proteins/gene expressions that contribute to chemical turbulence in cancer pattern formation).

Deep learning healthcare will allow AI (artificial intelligence)-assisted decision making in precision oncology with multi-omics data from patients (Esteva et al., 2019; Topol, 2019). Multi-omics can identify key GRNs critical in cell fate reprogramming in time-series (Silberbush et al., 2019; Yang et al., 2019). Unsupervised methods perform feature extraction and pattern recognition on newly presented cancer data while supervised learning methods classify cancer from non-cancerous data sets based on trained databases. Deep convolutional networks use multi-layered information processing and back-propagation to classify-predict complex signals such as images, speech and video data (LeCun et al., 2015). As discussed, fractal dimension analysis is a simple tool for distinguishing cancers from healthy tissues (Lennon et al. 2015) However, deep learning nets are revolutionizing clinical pathology analyses and medical imaging reconstruction as it incorporates many layers of neural network architectures coupled to machine learning algorithms (Shan et al., 2019; Zhang et al., 2019).

Three-dimensional live-cell imaging of patient-derived tumor organoids are used for single-cell fate tracking and karyotype sequencing to study CIN (chromosomal instabilities) (Bolhaquiero et al., 2019). There are molecular cytogenetic techniques, such as comparative genomic hybridization (CGH), Fluorescence in situ hybridization (FISH) *and* spectral karyotyping (SKY) that study how chromosomal aneuploidies affect gene expression profiles (transcriptome) and tumor heterogeneity (Wangsa et al., 2018). Hence, many techniques are emerging capable of simultaneously tracking chromosomal structure anomalies and single-cell gene expression patterns in cancer as dynamical systems. The coupling of deep learning to such data will revolutionize oncology.

Deep convolutional networks can assess complex drug interactions and are used for quality assessment of protein folding and protein structure prediction from sequence (Tong and Altman, 2009). Wavelet analysis, object detection and similar machine algorithms are employed by deep learning neural networks for pattern recognition on cancer imaging data. For instance, AlexNet and GoogleNet are examples of pre-trained convolutional neural networks performing image classification and with transfer learning can be trained on complex cancer tissues. Deep learning iteratively groups the features with clustering algorithms (e.g. k-means, t-SNE, isomap, etc.) and subsequently updates the weights of the network towards an energy minimum. In principle, this can be applied as unsupervised training to recognize chaotic patterns in cancer time-series gene expression profiles and time-lapse imaging. Hence, the P vs. NP problem herein asks: *Given Multi-omics map the cell fate transitions from stem cell populations, can Deep Learning nets find the minimum number of transcription factors and/or GRNs to reprogram cancer stem cells?* (Fard and Ragan, 2017; Palii et al., 2019)

For e.g. Deep learning nets cluster-classified the diverse subgroups in PDAC (pancreatic cancer) heterogeneity. Six molecular and clinically distinct subtypes of PDAC were identified with 160 subtype-specific markers (Zhao et al., 2018). Time series multi-omics data and machine learning is being used to predict metabolic pathways in cancer resistance (Castello and Martin, 2018). LC-MS (liquid chromatography-mass spectrometry) analysis of >30 cancer types show distinct metabolic drug targets (Li et al., 2019). Convergent cross-mapping with cytokine networks within the hematopoietic system was used to identify causal trajectories in regulatory transcriptional networks to construct a hierarchical, directed graph (Krieger et al., 2018). In a directed graph, the nodes are connected by flow arrows with

Preprints (www.preprints.org) | NOT PEER-REVIEWED | Posted: 27 June 2019 doi:10.20944/preprints201906.0288.v1

the weighting indicating their capacity. Deep learning can predict microsatellite instabilities in gastric cancers and thus improve immunotherapy decision in patients (Kather et al., 2019). Bayesian hierarchial clustering of heterogeneous stem cells with droplet Seq technology is feasible (Shun et al., 2019). These are merely few examples to illustrate oncology is transitioning towards deep learning healthcare and artificial intelligence-based patient care.

However, the most prominent of machine learning algorithms in the future of oncology is its applicability in dissecting the GRNs and reconstructing the Waddington energy landscape of cancer stem cells, thereby paving the route towards reprogramming cell fates (Saelens et al., 2019). The general approach to scRNA-Seq based cell lineage clustering and pseudotime inference is based on data filtering (pre-processing) and machine learning algorithms. CyTOF mass cytometry can be used for protein expression quantification in single cells (heterogeneity assessment of tissues), whereas RNA-Seq is used for observing differentially expressed genes in cells. The scRNA-Seq counts using the below-discussed algorithms are usually processed data. Hence, the raw data reads are filtered and selected for most differentially expressed genes in the cells. Single cell RNA Seq data is fed into the algorithms as a table/spreadsheet of cells (columns) by genes (rows) (i.e. expression matrix) followed by dimensionality reduction techniques like PCA (principal component analysis) or t-SNE, etc. Then, network-graph theoretic approaches are used to reconstruct the spatial neighborhood of cells with statistical inference (e.g. k means clustering (unsupervised) or KNN graph (supervised)). Following, optimization algorithms are used to find trajectories and regulatory modules. Correlation analysis (of activity over time or distance) assigns a score to potential gene-gene interactions, after unsupervised community detection algorithms and partial-information decomposition algorithms are employed. Dispersion cell -cell variability measures generally use covariance, correlation measures, Bayesian-statistical inference and Shannon entropy (mean entropy generally increases in transitions) (Chan et al., 2017) However, these methods can still be misleading as a lot of data filtering is done and information is lost. We assume cell to cell variability on the reduced latent components from high dimensional data, whereas spatiotemporal chaos can be extracted from the lost data. Low-gene expression levels can result in chaotic fluctuations in cell activity (i.e. sensitive dependence on small perturbations). For example, dynamics Bayesian network analysis is an algorithm, where given protein concentration changes in time, the factors most connected in the regulatory networks are determined to construct the circuitry. The discussed algorithms can be easily adapted to any data set, especially with transfer learning for large data sets (Stein-O'Brien et al., 2019).

Gene expression is for most part of literature considered as stochastic processes. An example, Piecewise-deterministic Markov processes (PDMPs) were shown to well-capture genetic switching in regulatory networks with the same performance measures as Monte Carlo approaches for large number of chemical kinetics. The probability (stochasticity) that a cell will move to the next microstate depended on how long it spent in the current macrostate (Lin et al., 2018). Gene expression variability increases during differentiation. These stochastic interpretations are not well understood and hence speculative. Moreover, they are model-system specific. Stochasticity may reflect 'flickering' when systems pass through a critical transition point, where the same definition holds for chaotic systems such as burst-like transition to turbulence (i.e. intermittency) (Stumpf et al., 2017).

Topslam estimates pseudotime by mapping Individual cells to the surface of a Waddington-like landscape with probabilistic dimensionality reduction (Bayesian Gaussian process latent variable model/GPLVM) (Zwiessele and Lawrence, 2017). These methods project high dimensional data into 2 or 3 components and distances are interpreted as cell-cell variability for cluster analysis and neighborhood

Preprints (www.preprints.org) | NOT PEER-REVIEWED | Posted: 27 June 2019 doi:10.20944/preprints201906.0288.v1

graphs. However, such machine learning methods are sensitive to fluctuations in gene expression data (environmental, intrinsic, etc.) and identify key regulators without understanding the system dynamics/complexity driven by molecular interactions (e.g. reaction diffusion patterns, epigenetic modifications, etc.).

Cell Router is a graph theoretic, flow network-based trajectory detection algorithm (Lummertz da Rocha et al. 2018). First, dimensionality reduction (PCA, t-SNE, Diffusion map, etc.), is performed on the single-cell data set. Following, a kNN Graph (k-Nearest neighborhood) is assessed. Then, the Jaccard similarity index finds the similarity between two cells (if they belong to the same cluster, high correlation) and the Louvain community detection algorithm configures the populations (assess weights of the graph by similarity of cell-cell) forming the flow network (source to sink directed graph to map the GRNs). The trajectories are found with Bellman-Ford algorithm (cost flow optimization algorithm) and ranked trajectories by total flow, cost and length (vertices). Then, the minimized trajectories are ranked by GRN scores (Pearson-Spearman correlation). Corresponding heat maps and dynamic curves of regulators are projected to obtain trajectories of the identified clusters displayed as a GRN flow network. Note: The Bellman-Ford algorithm computes the shortest paths from a single source vertex to all vertices in a weighted graph. It is slower than the Dijkstra's algorithm but can handle graphs with edge weights that are negative.

Seurat is another algorithm that can be used as a pre-processing tool of cancer data sets and the clusters can be further sorted using algorithms like CellRouter into flow networks. Seurat is a scRNA-Seq correlation and clustering computational tool (Butler et al., 2018). Seurat like CellRouter creates a flow network with similar algorithms. As discussed earlier, there is growing evidence challenging the hierarchial model of cancer stem cells. In argument, GBM shows that any cancer cell can be a stem cell depending on its microenvironment. ScRNA-Seq cell lineage and Waddington landscape reconstruction algorithms discussed herein can validate these claims.

Single **c**ell **E**nergy path (scEpath) is a method for mapping the quantitative energy landscape of single-cell dynamical processes. It reconstructs cell lineages and pseudotime (cell fate trajectory) inference with statistical-machine learning methods (Jin et al., 2018). scRNA-seq data is pre-processed/ filtered of low gene expressions, then using Spearman correlation of the adjacency matrix, builds a GRN, calculates the normalized energy between expressions, and performs a linear dimensionality reduction with PCA. Data then undergoes structural clustering of cells using an unsupervised framework called single-cell interpretation via multikernel learning (SIMLR). From the cell clusters, Boltzmann–Gibbs distributions are used to find the transition probabilities. To infer cell lineages, scEpath first constructs a probabilistic directed graph with maximum probability flow (equivalent to finding a minimum directed spanning tree (MDST) (Edmonds' algorithm)). Then, scEpath uses the R "princurve" package to fit a principal curve of these core cells (centroid) to compute the peudotimes (trajectories). The pre-processing is similar to Slingshot. Slingshot is a trajectory-cell lineage classification algorithm using dimensionality reduction techniques and cluster analysis (Street et al., 2018). Diffusion maps, PCA, etc. are used as dimensionality reduction followed by model-based clustering (expectation maximization/Bayes theorem) and k-means clustering and lastly MST (minimum spanning trees-Prim's algorithm) trajectories in inferring cell fate branching.

Hopfield (1982) pioneered the field of cybernetics. The Hopfield network is a recurrent neural network. Convolutional neural networks are tools for image classification and feature extraction/pattern recognition, whereas recurrent neural networks are typically useful in time-series analysis (Szedlak et al., 2014). Neural networks are being used in reconstructing Waddington landscapes from scRNA-Seq data.

Preprints (www.preprints.org) | NOT PEER-REVIEWED | Posted: 27 June 2019 doi:10.20944/preprints201906.0288.v1

Neural nets can perform hierarchial clustering on heterogeneous protein–protein (PPI) and protein–DNA interactions (PDI) datasets, with kNN supervised learning or unsupervised learning (on unlabelled data sets) including on cancer ecosystems (Lin et al., 2017).

Hopland is a continuous Hopfield neural network-based algorithm which interprets cell RNA-Seq or qPCR data for pseudo-time estimation and Waddington landscape reconstruction (Guo and Zheng, 2017). The Hopfield algorithm takes in the gene expression data and feeds it into the Hopfield network to construct the topography of the landscape with cell fate attractors based on gene to gene expression correlation. First, isomap dimensionality reduction is performed. Isomap generally consists of a kNN nearest neighborhood graph followed by geodesic (shortest path between two nodes) calculation from the Dijkstra's algorithm and multidimensional scaling. The fast-marching algorithm devised for solving the Eikonal equation (describes wavefront propagation in geometrical optics) was used to calculate the geodesic distances on the landscape as the weights of edges connecting the cells. Each gene is modelled as a neuron in the network, the cumulative energy values of which add up to each cell fate on the landscape. A Gaussian-mixture optimization algorithm was used to infer the parameters, the mean values of the outputs (gene expression values) from the cell lineages at different time points.

Gradient descent learning algorithm optimized the Hopfield (similar to backpropagation in Deep Learning) whereby the activation values (weights of the edges) undergo a relaxation process in the Lyapunov energy function. The Lyapunov energy function gives the energy values corresponding to the cell states (i.e. high energy corresponds to less differentiated states (hills) while low energy is differentiated states/energy minimization (valleys)). Cell differentiation paths follows the lowest potential energy in landscape in classical theory. However, cell fate fluctuations as seen in hybrids or complex adaptive systems such as cancer are not considered here. Hence, why strange attractors and chaotic fluctuations are proposed to better account for modelling cancer dynamics herein. Rather current approaches model the cell fate trajectory as a path integral/random walk between fixed, stable attractors. The Lyapunov energy function is given by:

$$E = -\frac{1}{2}\sum_{i=1}^{N}\sum_{j=1}^{N} W_{ij}U_iU_j + \sum_{i=1}^{N} I_iU_i + \sum_{i=1}^{N} \delta_i \int_0^{u_i} g^{-1}(u)du$$

Here g is the activation function (sigmoid in this case, yet can be ReLu, tanh, etc. such that it monotonically increases), $U_i = g_j(V_j)$, where V is the neuron outputs for N genes, W is the weights from gene expression data, δ_i is the gene signal degradation rate, I is the combination of propagation delays and regulations/noise from environment. Following, to simulate dynamic trajectories, Euler's method (1st order Runge-Kutta) is used to solve the updating of neurons as an ODE (ordinary differential equation) . To visualize the landscape topography, GPLVM is used (probabilistic nonlinear dimensionality reduction technique) onto a grid/stencil with a triangulated mesh, where the fast-marching algorithm computes the geodesics based on cell-cell variability in gene expression clusters and an MST algorithm identifies the minimum trees connecting clusters. Again, the efficiency of the algorithms discussed are model-dependent. For instance, Topslam outperformed Hopland in dissecting mouse embryo development, single cell RNA-Seq data without the Hopfield element (using only GPLVM and MST). Moreover, the data sets in these algorithms were highly filtered/processed. However, when there are so many algorithms inferring pseudotime of cell lineage branching, we must ask what is really happening at the level of cell fate transitions and decision-making, rather than fitting the data into limited models ?

In Netland/Hopland, the Runge-Kutta finite difference method is used to approximate ODEs and Euler Maruyama method for SDE (stochastic differential equations)/Langevin equations. These two

Preprints (www.preprints.org) | NOT PEER-REVIEWED | Posted: 27 June 2019 doi:10.20944/preprints201906.0288.v1

techniques apply for high molecular concentrations, whereas the Gillespie algorithm is used by the neural network for low copy number (i.e. categorized as stochastic fluctuations) (Guo et al., 2017).

The algorithms can be improved by adopting fluid dynamical grid systems- like LBM (lattice Boltzmann method) or FEM (finite elements method). Network-theoretic approaches to discretize fluid flow exist (Gustafson, 1984; Gustafson and Hartman, 1985). Neural network representation of FEM are theoretically established and hence available as pseudocodes that can be implemented into the above discussed algorithms (Takeuchi and Kosugi, 1994). Deep learning and machine learning algorithms (e.g. convolutional neural networks, fluid-grid based cluster analysis, etc.) that can model complex fluid flows is herein proposed as the solution to better model cell fate (Waddington landscape) reconstruction from time-series multi-omics data and time-lapse imaging of intracellular patterning. Thereby, in hypothesis, they can capture 'strange attractors' in cancer ecosystems at multi-scales (i.e. genes, proteins, cells, clusters).

The most advanced of current approaches in scRNA-Seq lineage reconstruction is scDeepCluster (Tian et al., 2019). scDeepCluster uses a model-based cluster analysis through multi-layered neural networks (i.e. deep learning) and hence outperforms the above-discussed algorithms. A finite element method (FEM) and Boltzmann/von Neumann machines in addition to deep learning can better capture fluid dynamical transitions in cell states. Moreover, scRNA-Seq technologies are rapidly improving with droplet-based microfluidics (e.g. Drop-seq). The lattice Boltzmann method is an efficient algorithm for mapping fluid turbulence and reaction diffusion systems (Chen and Doolen, 1998). Stochastic neural networks such as Boltzmann machines are simple fluid computers yet powerful tools to model fluid dynamics and complex wavefunctions (including many-body quantum systems). For e.g. the finite volume lattice Boltzmann method (FVLBM) based on cell center grids computes turbulent flow dynamics. An upwind discretization scheme for the method can thereby generate better pseudo-time calculations especially for complex diffusion-based mapping, especially if the flows are intermittent and chaotic.

Moreover, the optimization algorithm (e.g. Bellman-Ford, Dijkstra's or fast marching) discussed in the graph-theoretic flow networks herein can be replaced by Hamilton-Jacobi-Bellman (HJB) equations pertaining to fluid models (Farsikov et al., 2000). The solution of the Hamilton-Jacobi-Bellman equation is a partial differential equation that gives the optimal/minimum cost flow for a *dynamical* decision problem. HJB is a necessary and sufficient condition to find optimal time paths (i.e. finding local minima, attractors and singularities) of control variables in feedback loop systems (i.e. GRN). It is analogous to the Hamilton-Jacobi equation with the energy term minimized with respect to a weight-parameter w(t), given as

$$\frac{dS(q,t)}{dt} + \min\big(H(q,p,t;w)\big) = 0$$

Where, $p = \frac{dS}{sq}$, H is the Hamiltonian (energy), q and p are coordinates and momenta of the system, t is time and S is the Hamilton's principal function (upper limit of action integral). This is a complexity equation since min () adaptations are often (currently) intractable. Optimal control problems are generally nonlinear and without analytic solution, hence falling under the P vs. NP problem (i.e. cannot be resolved in reasonable time as in the current status of solving the Navier-Stokes smoothness and regularity). Therefore, BHJ is often handled with stochastic methods as is the case for all current computational methods in assessing cell fate decision making.

Preprints (www.preprints.org) | NOT PEER-REVIEWED | Posted: 27 June 2019 doi:10.20944/preprints201906.0288.v1

Current Waddington landscape reconstruction techniques do not account for intermittency and chaotic attractors (i.e. a cell fate fluctuates reversibly between otherwise point/fixed attractors in an apparently random manner). Hence, a Deep Learning net clustering algorithm consisting of CFD (computational fluid) techniques is proposed as the experimental approach to map the complex cell fate transitions and test for 'strange attractors' in the cancer Waddington landscape.

A few additional notes to keep in mind. Spurious attractors always emerge within the framework of a Hopfield network. These can correspond to Partially reprogrammed cell states (Lang et al. 2014). Simple Hopfield networks can map strange (hidden) attractors. With an activation function of tanh(x) to approximate the switches in timeseries trajectories, with as little as three or four neurons, strange attractors were mapped in the Hopfield (Li et al., 2005). The 3-Neuron Hopfield can exhibit chaotic attractors for different parameters as shown by its bifurcation plot and Lyapunov spectrum (Yang and Huang, 2016).

Another promising scope for machine learning is early detection of cancer through liquid biopsies. Machine learning algorithms applied on Intraoperative Raman spectroscopy can distinguish brain cancer stem cells from normal brain tissue (including both invasive and dense cancers) with an accuracy of 92%, sensitivity of 93%, and specificity of 91% (Jeremy et al., 2015). Background subtraction algorithms (e.g. roll ball algorithm) and autofluorescence algorithms are employed by such technique to characterize the cancer stem cell Raman bands from those of healthy tissues (Brusatori et al., 2017; Zhao et al., 2007). Machine learning can help assess liquid biopsies of patients, especially in the emerging field of exosome characterization. Cluster analysis and interpolation resolved Raman spectroscopy, post-purification of exosomes, found that cancer and healthy exosomes clustered differently in simple dimensionality reduction techniques like PCA (Gualerzi et al., 2017; 2019). The clustering also depends on the purity of the technique used to isolate them whereby analytical ultracentrifugation had less purity than column chromatography. Similarly, surface enhanced Raman scattering (SERS) signals of exosomes from normal and NSCLC (Non-small-cell lung carcinoma) cells was performed. The Raman spectroscopy patterns of cancerous exosomes by PCA showed unique peaks/Raman bands distinguishing NSCLC exosomes from healthy clusters (Shin et al., 2018). Other works using peak fitting algorithms, background subtraction methods and MCR-ALS algorithm (multivariate curve resolution- alternating least squares) with Raman spectral analysis to cluster-classify EV exosomes on gold-nanoparticle plated SERS substrates exist (Banaei et al., 2017; Shin et al., 2018). Such clustering methods can be implemented on the signals acquired from other spectroscopic methods as well and the distinguished spectral bands are potential biomarkers. For e.g. NMR (nuclear magnetic resonance) spectroscopy can detect exosomes (Ko et al., 2016). If the spectra show distinct bands for healthy exosomes vs. cancer-derived exosomes or they cluster differently in machine learning algorithms remains undetermined.

On a final note, a recent study showed that RNA MuTect found environmental mutagens generate many mutations in skin, lung and esophagus (i.e. air we breathe, our surrounding contact, the food we consume, etc.) in normal tissues, mostly in cancer promoting genes (Yizhak et al., 2019). This further raises questions about our lifestyle choices and environmental conditions. Moreover, this outlines the above-discussed methods can be implemented in many levels of oncology care (i.e. pre-clinical/preventative, diagnostic and prognostic/relapse).

TURBULENCE: THE BEGINNING

Turbulence is Universal. It occurs in all scales from the very large to the very small; within the astrophysical, geological, ecological, biochemical and quantum regimes. It is observed in the heat flow of

Preprints (www.preprints.org) | NOT PEER-REVIEWED | Posted: 27 June 2019 doi:10.20944/preprints201906.0288.v1

coffee cups, the motion of galaxies, flickering solar flares, gusts of wind, the swirls of Van Gogh's *The Starry Night*, pattern formation of clouds, predator-prey dynamics, blood flows in arteries, the dance of exosomes, airflow in the respiratory tract and the paintings of children (Lorenz, 1963; Wensink et al., 2012; Arts and Culture, 2019). Hence, turbulence also describes the flow of plastic pellets seeping into our oceans, the transmission of carcinogens in air, the vortex streets of cigarette smoke and the clouds of atmospheric pollutants.

For instance, the simulation of an ecological system was performed with three trophic levels: Nutrient, Prey and Predator, corresponding in the fluid system to laminar flow, turbulence and zonal flow respectively. Predator-prey dynamics were shown to be well characterized by intermittent puffs in a pipe for a turbulent fluid flow. The dynamics are driven by competition between different wavenumber (frequency) selection mechanisms and concluded to correspond to the Navier–Stokes equations (NSE) (Shih et al., 2016). Hence, the NSE equations are observed across all scales.

What is the NSE global regularity, smoothness and existence problem? The problem poses: Given an initial velocity vector, elucidate the existence of a velocity field and scalar pressure field which are both smooth and globally defined that solve the equations? Whether the Navier–Stokes equations allow solutions that develop singularities in finite time remains unresolved. However, there is immense body of experimental and theoretical works confirming- the topologies of turbulent flows consist of *strange attractors* (Ruelle, 1980; 1995; Landford, 1982; Miles, 1984; Brandstater and HL Swinney, 1987).

Leray (1934) showed the existence of weak (viscous) solutions of NSE in the sense of distributions satisfying the Cauchy-Schwarz energy inequality by spectral decomposition. According to L.F. Richardson, turbulent motion is a superposition of eddies undergoing an energy cascade (i.e. bifurcate into a fractal hierarchy of smaller eddies). The eddy size λ corresponds to a fluctuation of wavenumber $k \sim \frac{1}{\lambda}$. The structure of turbulence remains an unsolved problem. Experimentally, even the turbulence of smallest eddies is patchy and intermittent. Regardless, the $E(k)dk \sim \varepsilon^{2/3}k^{-5/3}dk$ (the Kolmogorov energy distribution) holds well with the spectra measured in experiments for low order moments where ε is the energy flux and E is the energy density (Kolmogorov, 1941). In experiments, turbulence arises in sudden large bursts, one after the other, followed by a period of relative quiescent behaviours (i.e. intermittency). Turbulent phenomena in fluids are characterized by strong fluctuations and power-law spectra suggestive of correlations observed in critical phase transitions (Goldenfeld, 2006).

In topological fluid dynamics, Moffat's theorem states that helicity (knottedness of vortex lines in a flow) can be interpreted as knot invariants (Arnold and Khesin, 1991; Ricco, 2000). That is, the vortex lines of turbulent flows form complex knotted structures (i.e. vortex tangles) that are stationary solutions to the Euler-Navier- Stokes equations and remains unchanged with transformation. *Theorem:* Suppose that t^*Is the largest time of existence of a smooth solution of the initial value problem for Euler's equation in R^3, then $\int_0^t max\,|\omega|(s)ds \to \infty\ as\ t \to t^*$, where ω is the vorticity (local rotation of a fluid). Consider the diffusion of the vortices in a turbulent flow given by the vorticity equation:

$$\frac{\boldsymbol{D\omega}}{\boldsymbol{Dt}} = (\boldsymbol{\omega} \cdot \boldsymbol{\nabla})\boldsymbol{u} + \boldsymbol{v}\boldsymbol{\nabla}^{\boldsymbol{2}}\boldsymbol{\omega}$$

Where v is the kinematic viscosity and u is the velocity, $\boldsymbol{\omega}$ is the vorticity defined as $\omega = \nabla \times u$ (i.e. Vorticity is the curl of the flow velocity vector u). In 2D, it is assumed ergodicity results in globally

Preprints (www.preprints.org) | NOT PEER-REVIEWED | Posted: 27 June 2019 doi:10.20944/preprints201906.0288.v1

smooth solutions to the initial value problem of Euler-NSE equations yet in 3D no analogous results are known due to the loss of regularity of initial data in finite time. Vorticity in 3D encounters a blow up as it becomes: $\frac{D\omega}{dt} = u \cdot \nabla\omega \rightarrow |\omega|\omega$ and the blow-up time becomes $\frac{1}{mod(\omega)}$.

Tao (2016) used logic gates and wavelet analysis to design a system of ODEs similar to NSE, and construct a blowup solution given the averaged version of Euler equations behaves like a von Neumann machine (a simple self-replicating computer used in fluid modelling). Blowup solutions for the Euler equations are known to exist for sufficiently small scaling exponents as may be the case for biosystem turbulences- low Reynolds systems. Current approaches consist of using deep learning neural networks and Boltzmann machines to model complex fluid flows (Kutz et al., 2017). Deep learning in fluid dynamics will pave better flow optimization techniques for the previously discussed graph-theoretic, cell fate reconstruction algorithms (Brunton et al., 2019). Whether 'quantum machine learning' algorithms can further elucidate the complexity of such problems remains theoretical (Sarma et al., 2019). Regardless, the fluid computers/machines discussed herein are tools that can be implemented in the Waddington landscape reconstruction from cancer stem cell, time-series datasets.

A decay function of time correlation is observed in experimental turbulence for which only for Axiom A diffeomorphisms it is proven that the intensity F(t) decreases exponentially at infinity (i.e. continuous frequency spectrum- which itself is the accumulation of large number of independent frequencies). This is a signature observed in all cases of experimental fluid turbulence. The frequency spectra (i.e. square amplitude of each frequency of a fluid) can detect strange attractors in the time evolution of the experimental system through attractor reconstruction methods and peak analysis. There is no direct test to 'sensitive dependence on initial condition' in hydrodynamics, hence, a frequency analysis of the fluid velocity (square amplitude vs. frequency) must be performed (Ruelle, 1973; 1995). These methods can be implemented on claimed systems of chemical turbulence in cell pattern formation.

Given the time-evolution of a fluid as a dissipative dynamical system, $\frac{d}{dt}X(t) = F_{\mu}\big(X(t)\big), X \in R^m$ where X is the state vector and F is the intensity function defined above, assume the bifurcation parameter μ is the Reynolds number. For small μ, steady state solutions exist while at larger μ, the oscillations asymptotically approach strange attractors (Ruelle, 1995). A small C^2 perturbation of a quasi-periodic flow on a 3-torus can produce strange axiom A attractors. An (ergodic) Axiom A attractor is non-trivial (strange) if it doesn't consist of a single periodic orbit and has a fractal dimension (Ruelle and Takens, 1971).

The competition between the inertial forces (velocity) and the viscous forces defines the Reynolds number. This presents a scaling problem as what Reynolds number produces turbulent flows varies from one system to another. The (normal) cell cytoplasm is often assumed to be dominated by viscous forces due to macromolecular crowding (i.e. cytoskeletal filaments, organelles, etc.) thereby limiting the movement of intracellular protein to Brownian motion. Note, if information on the initial/boundary conditions and all the dynamical forces acting upon the diffusing molecule are known, Brownian motion too is deterministic. Diffusion acts to redistribute the conserved quantities between neighboring compartments and phase-transition to chemical turbulences and long range orders (standing and traveling waves) far from onset of the (subcritical) lateral instability. Chemical turbulence in protein-mediated cell patterning was recently confirmed experimentally (Brauns et al., 2018).

The formation of cancers in organs and their metastases demonstrates a scaling over many orders of magnitude, from exosome flow to circulating tumor cells (CTC) in blood vessel/lymphatic networks. Such

Preprints (www.preprints.org) | NOT PEER-REVIEWED | Posted: 27 June 2019 doi:10.20944/preprints201906.0288.v1

biosystems comprise of multi-scale patterns of flow. For instance, at the organs level the Reynolds number may be around 1000, in the aorta up to 10,000, etc. (and depending on the pathophysiology the turbulence may increase to higher levels). Exosomes are in the nanoscale. Thereby, in principle, their flows must account for up to 1000-fold difference in Reynolds numbers than circulating tumor cells, in systemic flows. The Reynolds number is a dimensional analysis argument. In a cylindrical tube, whether we consider the length scale as the radius or diameter will change the Reynolds number by a factor of 2. The critical Reynolds number were shown to be in the order of 100-200 for Taylor-Couette and Rayleigh-Benard convection systems, which is relatively feasible in/around cellular biosystems (Ruelle, 2012; 2014).

Systemic circulation exhibits turbulence yet the turbulent kinetic energy increases with ageing and pathophysiologies (Hojin et al., 2018). Understanding how the strange attractor dynamics change from one pathophysiology to another is thereby a clinical diagnostic tool. As seen, simplifications of NSE like Darcy's law and reaction-diffusion equations are currently used in describing tumor flows. Mapping cancer pattern formation as strange attractors, allows the study of how these attractors change under therapeutic interventions and in principle, find the attractors for reprogramming cancer cell fates.

Hematopoietic iPSC (induced pluripotent) stem cells were shown to increase their production rates in systemic flows by many orders of magnitude under turbulence (Ito et al., 2018). Hence, such mechanisms may be utilized by cancer stem cells to undergo rapid clonal expansion during metastatic flow. Given the cancer microenvironment consists of intermittent flows, it remains to be elucidated whether turbulence allow cancer microenvironments to increase exosomes shedding in the formation of distant pre-metastatic niches. However, current findings only support that the information content/cargo of the oncosomes (i.e. oncoproteins, miRNA, etc.) and their concentration alone changes in disease progression.

Cancer metastasis, growth and therapy response is governed by fluid dynamics (Koumoutsakos et al., 2013; Goetz, 2018). Using shear-stress tensor in terms of viscosity and the fluid velocity gradients, focal adhesion dynamics can be investigated in cancer metastasis (Thamilselvan and Basson, 2004; Chivucula et al., 2014). The hemodynamic shear forces modulate the formation and location of pre-metastatic niches through regulating CTC flow. Microfluidic experiments on 3D ovarian cancer models show that fluidic streams induce a motile and aggressive tumor phenotype. Hence, higher fluid flow were shown to induce EMT transitions and promotes aggressive phenotypes that can metastasize (Rizvi et al., 2013; Ketene et al., 2012). Furthermore, Huang et al. (2018) showed that non-laminar (turbulent) shear stress may increase the adhesive ability of cancer cells in metastatic invasion. Note: Microfluidic devices/flow chambers are reshaping experiments on tumor dynamics (i.e. lab/organ on a chip). For instance, carcinogen exposure from food (gastric juices) or cigarette smoke can be mimicked on layers of patient-derived gastric or lung cancer cells in the chip. Videomicroscopy can map the dynamics along with appropriate biochemical techniques (e.g. flow cytometry and RNA-Seq) to profile the adaptive changes. Exosomes profiling can also be performed in vitro. Drug screening can also be performed.

Blood flow is often modelled using the Hagen-Poiseuille equation assuming vessels to be cylindrical pipes and incoming flows to be laminar. However, tumor vasculature does not conform to this naïve assumption and most biological fluids are anisotropic/non-Newtonian. The complexity of tumor vasculature and tissue organization can be quantified in terms of fractal dimensions, where such blood vessels showed only intermittent flows (Jain and Baish, 1998; Nasu et al., 1999). Mutifractals is a tool to study the geometry of turbulence (Sreenivasan and Meneveau, 1986; 1991). Hence, the application of

Preprints (www.preprints.org) | NOT PEER-REVIEWED | Posted: 27 June 2019 doi:10.20944/preprints201906.0288.v1

Box counting algorithms on tumor vasculature and morphology can study how treatments alter its geometric complexity (Coffey, 1998; Yakhota and Sreenivasan, 2004).

The fluid shear stresses experienced by CTC cells consist of turbulence. Blood flow velocities in the circulation system can range from 0.03 to 40 cm/s depending on the vessel size. How individual CTCs and CTC emboli can withstand these intercellular interactions and persist in the fluid flow is not yet fully understood. However, the Navier-Stokes equations are imposed on Cartesian fluid grids in current approaches and the fluid velocities must be solved to measure CTC dynamics. The blood plasma is modeled as a viscous, incompressible Newtonian fluid governed by Navier-Stokes equations (Rejniak et al., 2016). With appropriate boundary conditions, the steady, incompressible Navier-Stokes and continuity equations governing the flow are solved using finite-volume CFD (computational fluid dynamics) to model circulating melanoma cells and their adhesion dynamics (Behr et al., 2015). Doppler techniques can track turbulent blood flow detected in liver tumor patients in the hepatic vein portal where the most malignant tumors had greater turbulence (Yasuhara et al., 1997).

Levinthal's paradox states protein folding is an NP problem with a puzzling time scale. Although misfolded aggregates have long range interactions with many protein complexes and are aided by chaperones, protein folding displays combinatorial complexity yet nature resolves it within seconds. Recent evidences show protein folding may best be described by the turbulence of Kolmogorov-Richardson's energy cascade, where turbulent eddies and vortices breakdown into smaller fractal hierarchies. The protein folding flows of an SH3 domain protein model have fractal nature and are filled with 3D eddies containing strange attractors, at which the tracer flow paths behave as saddle trajectories (Kalgin and Chekmarev, 2011; Andryushchenko and Chekmarev, 2017). The SH3 domains are crucial in focal adhesion complexes regulating cancer metastasis and EMT transitions. Folding dynamics of villin subdomain HP-35 protein in a FRET experiment was shown to obey the β-model of turbulence with many orders of turbulent flow transitions for eddies in the 3D conformational space (Andryushchenko and Chekmarev, 2016; Chekmarev, 2018).

Turbulence has been observed in bacterial swarming and the collective dynamics of cellular microorganisms. Active fluids are a rapidly evolving research field inspired by the biophysics of dense suspensions of motile cells (Dunkel et al., 2013). Their hydrodynamic interactions give rise to the emergence of meso-scale vortex patterns reminiscent of two-dimensional turbulence. Cell tissues and reconstituted cytoskeletal solutions exhibit active turbulence where emergent scaling behaviours were observed. Bundles of microtubules and their associated kinesin motors deposited on an oil–water interface behaved like 3D vortex tangles in a turbulent fluid (Sumino et al., 2012). 2D distortions of nematics consisting of microtubules show quadratic variants of the Navier-Stokes equations in growth (Martinez-Pratt et al. 2019). Self propelled particles like cytoskeletal flocking, follow continuum mechanics like fluids and can exhibit turbulence even at low Reynolds (Marchetti et al., 2013; Baggaley, 2016). Active fluids such as actin and microtubules can be described using the Navier-Stokes equations (James et al. 2018[a,b]). Coupling a mass-conserved Turing-like reaction–diffusion system for polarity proteins to an active-gel description of the actomyosin cortex, revealed active turbulence in *C. elegans* embryos (Gross et al., 2019) Hence, the emerging field of soft-matter nematics shows turbulence can occur at low Reynolds number making the NSE problem more difficult (Doostmohammadi et al., 2018).

Cell division is orchestrated by intracellular protein patterning, mainly from cytoskeletal filaments and cell polarity complexes. Abnormal cell division is the signature of cancer. Usually low intracellular concentration of proteins and their corresponding dynamics are modelled as stochastic fluctuations.

Preprints (www.preprints.org) | NOT PEER-REVIEWED | Posted: 27 June 2019 doi:10.20944/preprints201906.0288.v1

Classical theory states these chemical systems are close to equilibrium and inertial effects are negligible. However, a recent theory by Halatek and Frey (2018) challenged the dogma and using finite elements method (FEM) simulations predicted chemical turbulence (spatiotemporal chaos) at the onset of the pattern-forming instabilities in tissues. Cytosolic diffusion constant D_c were in the order of 60 $\mu m^2 s^{-1}$ in 1D, where the MinD-ATP/ADP in bulk were given by the reaction-diffusion equations:

$$\partial_t u_D(z,t) = D_c \nabla_z^2 u_D - F_{u_D}$$

$$\partial_t u_T(z,t) = D_c \nabla_z^2 u_T + F_{u_D}$$

u_D and u_T define the cytosolic density of MinD- ATP/ADP conformations and assume the MinD-ATP binds to the membrane via nonlinear coupling rate constants. The resultant kymograms demonstrated *turbulent flows at low MinE/MinD ratios*. Usually low-levels of gene expression patterns, protein concentrations or signal fluctuations (e.g. in RNA Seq) are filtered out in the algorithms computing the cell lineage tracking as discussed earlier. Hence, the strange attractors may be relevant to the low-level protein fluctuations otherwise classified as 'noise'.

The theoretical predictions of Halatek and Frey (2018) have been confirmed experimentally (Denk et al., 2018). This must be experimentally repeated in the PAR cell polarity complexes (the mammalian equivalence of the Min proteins) and other associated cytoskeletal remodelling proteins (e.g. cdc42-RhoGTPases/Rac system of actomyosin contractility and focal adhesion dynamics with ECM) in cancer (stem) cells during cell fate bifurcations. According to these findings, chemical turbulence in pattern formation is used as a synonym for spatio-temporal chaos, i.e. a broad distribution in the power spectrum and a low spatial correlation length reminiscent of the Kolmogorov spectrum. But none of these terms are strictly/unambiguously defined in the literature. The term was adapted from the work by Nobel laureate Gerhard Ertl on reactions of heterogeneous catalysis (Kim et al., 2001). According to this work, during chemical turbulence, both the amplitude and the phase of local concentration oscillations are strongly fluctuating creating spiral waves as seen in the Denk et al. (2018) data with Min proteins. This diffusion-induced turbulence is typical for oscillatory surface chemical reactions and has been observed under special conditions in the Belousov-Zhabotinsky reaction (Kim et al., 2001). Hence, turbulent chemical oscillations can occur in patterning (reaction-diffusion) systems (Mecke, 1996). The Belousov-Zhabotinsky reaction is often a toy-model system for turbulent pattern formations (Ouyang and Swinney, 1991; Ruelle, 1995).

Turbulence was treated as a heat flow problem using nonequilibrium statistical mechanics of moving fluid particles in three-dimensional lattice boxes (Ruelle, 2012). As mentioned, the Reynold's number is not a well-defined quantity. Consider

$$\boldsymbol{\zeta}_p = \frac{p}{3} - \frac{1}{lnk} ln\Gamma\left(\frac{\mathrm{p}}{3} + 1\right)$$

Where $\boldsymbol{\zeta}_p$ is the intermittency exponent, Γ is the gamma function, P/3 is the Kolmogorov term and $(\ln k)^{-1} \sim 0.32$. The average change in velocity $\vec{u}$ over the small length of a turbulent fluid in these boxes is roughly

$$\langle |\Delta \vec{u}|^p \rangle \sim l^{\zeta_p}$$

Thus, we see the onset of turbulence below a Reynolds number of ~100 with numerical methods (independent of geometry) (Ruelle, 2012). Then, the macroscopic fluid transitions on the grid system are

Preprints (www.preprints.org) | NOT PEER-REVIEWED | Posted: 27 June 2019 doi:10.20944/preprints201906.0288.v1

given by Boltzmann-Gibbs distributions. Hence, the probability distribution of turbulent eddies in a lattice cube and their lifetimes gives the canonical distribution:

$$\rho(E) \sim \exp(-\beta |u_n|^3) d^3 u_n$$

Using the second law of thermodynamics we get the state transition from an attractor A to B as:

$$\frac{\rho(A \to B)}{\rho(B \to A)} \geq \exp[-\langle \Delta S \rangle - \beta \langle \Delta Q \rangle] \therefore \rho \sim \exp(-\beta \Delta G)$$

Where ΔQ is the heat enthalpy transferred to the active heat bath, β is the coldness of the system ($\frac{1}{k_B T}$), S is the entropy and G is the Gibbs free energy. Such a description well applies to the metastable cell states of the Waddington attractor landscape (Ruelle, 2012).

On a final note, machine/deep learning in the modelling of complex fluid flows like turbulence may also help resolve other current pediatric health issues in North America. For e.g. video recordings of crowd disasters reveal sudden transitions from laminar to "turbulent" flows near the time of accidents, by modelling the motion of people as many-particle fluids. This may help explain traffic flow analyses and other self-organized (social) network dynamics (Helbing et al., 2007). In theory, deep learning convolutional neural networks and machine learning algorithms can analyze video motion of traffic flows and dissect patterns in their fluid dynamics. Moreover, deep learning-assessments must be made on how environmental factors contribute to cancer epidemiology (e.g. video recordings of air pollution flow).

QUANTUM CHAOS

Quantum chaos is the quantum description of classically chaotic systems. Although fundamentally all processes are quantum dynamic, a newly emerging field called *quantum biology* proposes that biosystems may exhibit macroscopic quantum effects at ambient temperature (Lambert et al., 2012). The most controversial postulate of this field, yet most pertinent to cancer, is the plausibility of nonlocal information processing in microtubule networks (Hameroff and Penrose, 2014). There is a lack of rigorous experimental evidence to support these claims. However, recently it was shown, thermal fluctuations are sufficient to remodel microtubule lattices' dissipative dynamics. The growth not only occurs on the extremities as previously thought but dimers can be added anywhere in the entire rod (Shaedel et al., 2019). The tetrapolar spindle generated through cytokinesis defects are used in cancer as a transitory/intermediate state on the route to aneuploidy and genetic diversification in cell division (Lens and Medema, 2019).

Biological systems (especially on nanoscales and below), show there exists processes for which a quantum mechanical description is necessary to fully characterize the behaviour of the relevant subsystem (Marais et al., 2018; McFadden and Al-Khalili, 2018). If further validated, certain proteins in cancer cell patterning, cytoskeletal filaments in cell division (cause of aneuploidy/CIN) and exosome flows are few examples pertaining to the scales at which such macroscopic quantum effects can apply.

Preprints (www.preprints.org) | NOT PEER-REVIEWED | Posted: 27 June 2019 doi:10.20944/preprints201906.0288.v1

Quantum coherent beatings are detected in photosynthetic systems for femtoseconds in the FMO (*Fenna-Matthews-Olson*) complex suggesting energy transfer is best described as a linear superposition of chromophores energy states (Engel et al., 2007; Thyrhaug et al., 2018). Craddock et al. (2014) propose a longer coherence time occurs for the Tryptophan (Trp) networks in tubulin via Forster dipole–dipole energy transfer, forming coherent beats at 600 fs. Forster resonance energy transfer (FRET) via dipole-dipole coupling of Trp is predicted as the mechanism responsible for the extended quantum coherence and other nonlocal effects in microtubule networks at ambient temperature.

Frohlich (1968) proposed that a set of biological oscillators can condense to the lowest frequency vibrational mode by the supply of biochemical energy, which he defined as *pumped phonons*. The pumped phonons are predicted by some to account for the plausibility of macroscopic quantum effects in microtubules in 4 or 5 orders of magnitude of self-similar (fractal) organization (Hameroff and Penrose, 2014). Davydov (1985) tried to find spatial localization of such low-frequency vibrational energy using solitons in DNA, proteins, etc. while Frohlich sought for frequency selection. Recent experimental evidences are suggesting long-range, long-lived coherence of low frequency vibrational modes in protein structures due to Frohlich-like condensation in the hen-egg white lysozymes (Lundholm et al., 2015).Given the phosphorylation energy of GTP hydrolysis at MAPs (microtubule-associated proteins) binding site, simulations of microtubules as coherent phonons suggest that phonon maxima correspond to MAP binding sites (Prodan and Prodan, 2009). Raman spectroscopy of metabolically active (*E. coli*) cells claimed to have measured such coherent vibrations as well (Del Giudice et al., 1982). Recent evidence suggests Rabi oscillator-like quantum entanglement can be observed in bacteria (Marletto, 2018).

Solving the Navier-Stokes equations (NSE) is a complexity problem. Quantum mechanics has fluid-like properties and hence is interconnected to the NSE problem. Although quantum machine learning may help infer approximate solutions to the NSE, both quantum mechanics and turbulence can only be understood by exploring the underlying complexity of fluid topologies (i.e. vortex tangles). There are alternative formulations of quantum mechanics by Madelung, de Broglie and Bohm that describes nature in terms of fluid dynamics (Madelung, 1927; Bohm, 1952; de Broglie, 1987). The Hamilton-Jacobi equations is the closest formulation of classical mechanics where the motion of a particle can be represented as a wave (i.e. transition to quantum mechanics). The de Broglie-Bohm theory depicts the Schrodinger wave equation as modified Hamilton-Jacobi equations and thereby allow a quantum analogue of the Navier-Stokes equations (Harvey, 1965; Bohm and Hiley, 1995). Cosmological models such as SVT (superfluid vacuum theory), superfluid dark matter, etc. propose the fundamental constituent of space-time geometry as a fluid. Such fluid interpretations of quantum theory allow the emergence of macroscopic quantum effects.

Bohm metaphorically interprets the fabric of reality as a multi-dimensional ocean known as the Holomovement (Bohm, 1980). Note: The Waddington landscape is a metaphor too. Turbulence in the quantum scale consists of complex vortex tangles, interwoven knots, loops and strings (i.e. topologies observed in current theoretical approaches to quantum gravity such as Loop quantum gravity and string theory) (Baggaley et al., 2012). Topological fluid dynamics and braids theory address the same problems in classical scales. Hence, an understanding of turbulence is a foundational, multi-scale problem.

The Madelung hydrodynamics equations are quantum Euler equations:

$$\frac{du}{dt} = \frac{\partial u}{\partial t} + u \cdot \nabla u = -\frac{1}{m}\nabla(Q + V)$$

Preprints (www.preprints.org) | NOT PEER-REVIEWED | Posted: 27 June 2019 doi:10.20944/preprints201906.0288.v1

The Madelung transformation (1927) and de Broglie-Bohm theory allows the Schrodinger equation to be in hydrodynamic form. Given the polar form of the wavefunction $\psi(x,t) = R(x,t)e^{\frac{iS(x,t)}{\hbar}}$, and respecting the conservation of probability (fluid density): $\partial\rho(t) + \nabla(\rho u) = 0$, by substituting the Schrodinger equation we derive $\frac{\partial S}{\partial t} + \frac{1}{2}mu^2 + Q(x,t) + V(x,t) = 0$, where $u(x,t)$ is the quantized velocity of the (probability) fluid, $\rho = m|\Psi|^2$ is the fluid (probability) density, m is the mass of the fluid system, $R = \sqrt{\rho}$ the amplitude of ψ, S is the phase of the fluid wavefunction (also pertains to the action S in Feynman path integral formulation) and Q is Bohm's Quantum potential (Holland, 1993; Bohm and Hiley, 1995), given by:

$$Q = -\frac{\hbar^2}{2m}\frac{\nabla^2\sqrt{\rho}}{\sqrt{\rho}}$$

The expectation value (most probable value) of the quantum potential is then $\langle Q\rangle = \langle\frac{1}{2}[\frac{\hbar}{2\mathrm{m}}\nabla(\ln\rho)]^2\rangle = \frac{1}{2}(\frac{\hbar}{2\mathrm{m}})^2 I$, where I is the Fisher information given as $I = \int\frac{1}{\rho}(\nabla\rho)^2 dv = \int\rho[\nabla(\ln\rho)]^2 dv$. The Pressure tensor P is related to the Quantum potential by their respective gradients: $\frac{\nabla P}{\rho} = -\nabla Q$ (Caldeira and Leggett, 1983; Jungel et al., 2011). The fluid flow is quantized and only accepts solutions of discrete vortices given by

$$\oint u\cdot dl = 2\pi\hbar\mathrm{n}$$

where u is the velocity field and the solutions $u(x,t) = \frac{\nabla S(x,t)}{m}$ are integer quantized (n=0,1,2,3,…). Note how the hydrodynamic description of quantum mechanics allows probabilities to be viewed as fluid densities, thereby deviating from the conventional probabilistic interpretation towards one of *deterministic chaos*.

Most biomolecules are tuned at the edge of chaos/transition point e.g. cell membrane fluidity. Power law decay is seen across spontaneous symmetry-breaking and self-organization processes in biosystems. Such emergent behaviours are termed 'edge of criticality' processes. Vattay et al. (2014) demonstrated that the transition from quantum to classical chaos is best described as a power law decay. Some biological systems can stay quantum coherent for long time at room temperature near critical quantum chaos. The decoherence exhibits a power law decay as opposed to exponential decay where above the critical point, chaotic dynamics emerge (Vattay et al., 2014).

Most biological networks are close to being scale-free, where their node connectivities follow a power law, i.e. the probability that a node is connected with k other nodes (the degree distribution p(k) of a network) decays as a power law. Systems that are fine-tuned at the critical transition point can withstand environmental decoherence and thereby permit long-lived coherence and transport to coexist for several scales/orders of magnitude. Such processes are observed in the newly emerging field of *quantum biology* (e.g. photosynthetic energy transfer of FMO complexes, magnetoreception of birds, tunneling in DNA, etc.) (Lambert et al., 2012).

Furthermore, Vattay et al. (2015) used a fractal-box counting method to compute multifractal wavefunctions for proteins (e.g. myoglobin) describing the energy level statistics with the extended Huckel model and random matrix theory. Moreover, experiments of millimetric fluid droplets on vibrating fluid baths show the droplet walkers exhibit chaotic fluid motions. The collective ensembles exhibit quantum mechanical properties similar to those of the double slit experiment's interference patterns (Harris and Bush, 2013; Moláček and Bush, 2013;). Hence, evidences show macroscopic

quantum hydrodynamics can be experimentally conceived supporting the pilot wave theory (i.e. fluid dynamical interpretations of quantum mechanics) (Bush, 2015).

CONCLUSION

The discussed mathematical tools of machine/deep learning, graph theory and experimental fluid dynamics will pave the future of dynamical therapies in oncology and in principle, approach 'cancer reprogramming'. Deep-learning cluster algorithms based on gridding schemes compatible with computational fluid dynamics (e.g. FEM, LBM, Boltzmann or von Neumann machines) are proposed as means of testing for 'strange attractors' and mapping complex flow transitions in cancer cell fates. Time-series multi-omics data (scRNA-Seq) and time-lapse imaging of identified intracellular protein patterning (i.e. differentiation maps with reporters) in cancer stem cells are proposed as ideal data sets to test the presence of strange attractors.

"Children are the greatest teachers of turbulence; do observe them paint. Cancer is not cells in a petri dish nor an experimental system. She/He talks, dances, and smiles."

"Big whorls have little whorls Which feed on their velocity, And little whorls have lesser whorls And so on to viscosity"- L.F. Richardson (1922)

ACKNOWLEDGEMENTS

Thanks to Dr. Mario D'Amico (Concordia University), Dr. Rolando Del Maestro, Dr. Arena Goffredo, Dr. Mohamed Abdouh, and Dr. Lorenzo Ferri of McGill University for granting me the knowledge and tools discussed herein.

DECLARATIONS: I, Abicumaran Uthamacumaran, am the sole author of the submitted paper. There are no competing interests.

REFERENCES

- Kelly Oakes. Nearly half of all global childhood cancer cases go undiagnosed. Nature News. (13, March, 2019).
- Leukemia and Lymphoma Society.https://www.lls.org/leukemia/acute-lymphoblastic-leukemia/diagnosis/all-subtypes
- https://www.cancer.org/cancer/leukemia-in-children/detection-diagnosis-staging/prognostic-factors.html
- Gaiti, F. et al. Epigenetic evolution and lineage histories of chronic lymphocytic leukemia. Nature. 569(7757):576-580 (2019)
- Boer, JM and den Boer ML,. BCR-ABL1-like acute lymphoblastic leukaemia: From bench to bedside. Eur J Cancer. 82:203-218 (2017)
- Bhojwani, D et al. "ETV6-RUNX1-positive childhood acute lymphoblastic leukemia: improved outcome with contemporary therapy." *Leukemia* vol. 26,2 (2012)
- Collins, V Peter et al. Pilocytic astrocytoma: pathology, molecular mechanisms and markers. *Acta neuropathologica* vol. 129,6 (2015): 775-88

- Verhaak, R.G. et al. Integrated genomic analysis identifies clinically relevant subtypes of glioblastoma characterized by abnormalities in PDGFRA, IDH1, EGFR and NF1. Cancer Cell. 17, 98-110 (2010)
- M. Ceccarelli et al. Molecular profiling reveals biologically discrete subsets and pathways of progression in diffuse glioma. Cell 164(3):550-563 (2016)
- EA. Sweet-Cordero and J.A. Biegel. The genomic landscape of pediatric cancers: implications for diagnosis and treatment. Science, 363:6432. Pp. 1170-1175 (2019)
- Staedtke, V. et al. (2016). Actionable molecular biomarkers in primary brain tumors. Trends Cancer 2, 338-349.
- Azzarelli, R. et al. "The developmental origin of brain tumours: a cellular and molecular framework." *Development (Cambridge, England)* vol. 145,10 dev162693. (2018)
- Bai, Hanwen et al. "Integrated genomic characterization of IDH1-mutant glioma malignant progression." *Nature genetics* vol. 48,1 (2016): 59-66.
- V Korber et al. Evolutionary trajectories of IDH-wildtype glioblastomas reveal a common path of early tumorigenesis instigated years ahead of initial diagnosis. Cancer Cell, 35(4):692-704.e12. (2019)
- Barthel et al. Systemic analysis of telomere length and somatic alterations in 21 cancer types. Nat genetics. 2017
- Doomed from the TERT? A two-stage model of tumorigenesis in IDH-wild-type glioblastoma. L.F. Stead and R.G.W. Verhaak. Cancer Cell. 35(4):542-544 (2019)
- Del Maestro, R. Surgical resection and glioblastoma: molecular profiling and safety. Can J Neurol Sci, 39:561-562 (2012)
- Dea, N, Fournier-Gosselin, MP, Mathieu, D, Goffaux, P, Fortin, D. Does extent of resection impact survival in patients bearing glioblastoma? *Can J Neurol Sci*. 2012;39(5):632–7
- Klughammer, J., et al. The DNA methylation landscape of glioblastoma disease progression shows extensive heterogeneity in time and space. *Nat. Med.* 24(10):1611-1624 (2018)
- Filbin M and Monje, M. Developmental origins and emerging therapeutic opportunities for childhood cancer. Nat. Med 25: 367–376. 2019
- M.G. Filbin et al., Developmental and oncogenic programs in H3K27M gliomas dissected by single-cell RNA-seq. Science. Vol. 360, Issue 6386, pp. 331-335 (2018)
- The cancer genome atlas research network Comprehensive genomic characterization defines human glioblastoma genes and core pathways. Nat. 455: 1061-1068 (2008)
- Salloum R et al. Characterizing temporal genomic heterogeneity in pediatric high-grade gliomas. Acta Neuropathol Commun. 5(1):78 (2017)
- Det, C. et al. DNA methylation-based classification of central nervous system tumours. Nature. 2018 Mar 22;555(7697):469-474 (2018)
- A Mackey et al. Integrated molecular meta-analysis of 1000 Pediatric high-grade and diffusive intrinsic pontine glioma. Cancer cell. 32(4): 520-537 (2017)
- Zhao, J. et al. Immune and genomic correlates of response to anti-PD-1 immunotherapy in glioblastoma. Nat. Med. 2019
- Macleod, G. et al. Genome wide CRISPR-Cas 9 screens expose genetic vulnerabilities and mechanisms of Temozolomide sensitivity in Glioblastoma stem cells. Cell Rep. 27(3):971-986 (2019)

- Murayi, Roger, and Prashant Chittiboina. “Glucocorticoids in the management of peritumoral brain edema: a review of molecular mechanisms.” Child's nervous system: ChNS : official journal of the International Society for Pediatric Neurosurgery vol. 32,12 (2016): 2293-2302.
- Clarson, CL and Del Maestro, RF. Growth failure after treatment of pediatric brain tumors. Pediatrics 103(3):E37 (1999)
- S.L. Liauw et al., New paradigms and future challenges in radiation oncology: an update of biological targets and technology. Sci Trans Medicine. 5(173 (2013)
- Cools-Lartigue, J. et al. Neutrophil extracellular traps sequester circulating tumor cells (CTC) and promote metastasis. J Clin. Investigation. 123(8): 3446-3458 (2013)
- Keklikogolu, I. et al. Chemotherapy elicits pro-metastatic extracellular vesicles in breast cancer models. Nat cell Biol. 21:190-202 (2019)
- Stewart, P.A. et al., The effect of cellular microenvironment on vessels in the brain. Part 1: Vessel structure in tumor, peritumour, and brain from humans with malignant glioma. Int J Rad Biol 60(1/2):125-130 (1991)
- Corcoran A. & del Maestro, R. Testing the "Go or Grow" hypothesis in human medulloblastoma cell lines in two and three dimensions. Neurosurgery. 2003 Jul;53(1):174-84; discussion 184-5.
- M.C. Vladoiu et al. Childhood cerebellar tumors mirror conserved fetal transcriptional programs. Nat. 2019
- Sunayama, J. et al. Dual blocking of mTor and PI3K elicits a prodifferentiation effect on glioblastoma stem-like cells. *Neuro-Oncology. 12(12):1205-1219 (2015)*
- Suvà, M.L., Riggi, N., & Bernstein, B.E. Epigenetic Reprogramming in Cancer. Science 339.6127 (2013)
- Suva, M.L. et al. Reconstructing and reprogramming the tumor propagating potential of glioblastoma stem-like cells. Cell. 157(3): 580–594 (2014)
- D.M. Taylor et al., The Pediatric Cell Atlas: Defining the Growth Phase of Human Development at Single-Cell Resolution. Developmental Cell 49 (2019)
- Canadian Cancer Society. www.cancer.ca/en/cancer-information/cancer-101/childhood-cancer-statistics/?region=on
- Yanchar, N. L., Warda, L. J., & Fuselli, P. Child and youth injury prevention: A public health approach. Paediatrics & child health, *17*(9) (2012)
- Health Canada; Mental Health Commission of Canada. Children and youth. [cited 2018 Jul]. Available from: https://www.mentalhealthcommission.ca/English/what-wedo/children-and-youth (2018)
- Waddington, C.H. The Canalization of development and the inheritance of acquired characters. Nature 150, 563–565 (1942)
- A deterministic map of Waddington’s epigenetic landscape for cell fate specification, S Bhattacharya et al. BMC Systems Biol. 2011, 5:85
- Quantifying the Waddington landscape and biological path for development and differentiation J Wang et al. PNAS 108 (20):8257 -8262 (2011)
- J Davila-Vederrain, 2015. Modelling the epigenetic attractors landscape: toward a post-genomic mechanistic understanding of development. Front. Genet. (2018)
- Zhou JX, Pisco AO, Qian H, Huang S (2014) Nonequilibrium Population Dynamics of Phenotype Conversion of Cancer Cells. PLoS ONE 9(12): e110714.

- Perkins, T.J., Foxall, E., Glass, L., & Edwards, R., et al., A scaling law for random walks on networks. Nat. Comm. 5:5121 (2014)
- Lorenz, E.N. Deterministic nonperiodic flow. J. Atm. Sci. 20:130-141 (1963)
- Elowitz, MB. Stochastic gene expression in a single cell. Science. 297(5584):1183-6 (2002)
- Wang, J. Landscape and flux theory of nonequilibrium dynamical systems with applications to biology. Adv Phys. 1-137, 64(1) (2015)
- Li, Chunhe and Jin Wang. Quantifying cell fate decisions for differentiation and reprogramming of a human stem cell network: landscape and biological paths. *PLoS computational biology* vol. 9,8: e1003165 (2013)
- Wang, J. et al. 2010 the potential landscape of genetic circuits imposes the arrow of time in stem cell differentiation. Biophys J. 99, 29-39
- Li, Q. et al. Dynamics inside the cancer cell attractor reveal cell heterogeneity, limits of stability, and escape. PNAS. 113 (10) 2672-2677 (2016)
- Mojtahedi M. et al. (2016) Cell Fate Decision as High-Dimensional Critical State Transition. PLoS Biol 14(12): e2000640
- Ruelle, D. Turbulence, strange attractors and chaos. World Scientific Ser A. 16. (1995)
- Huang S and Kauffman, S. 2013. How to escape the cancer attractor: rationale and limitations of multi-target drugs. Semin Cancer Biol. 23(4): 270-278
- Font-Clos, F. Topography of epithelial-mesenchymal plasticity. PNAS. 1-6 (2018)
- Kauffman, S.; Levin, S. (1987). "Towards a general theory of adaptive walks on rugged landscapes". Journal of Theoretical Biology. 128 (1): 11–45
- Weinberger, Edward "Local properties of Kauffman's N-k model: A tunably rugged energy landscape". Physical Review A. 10. 44: 6399–6413. (1991)
- M Mezard and A Montanari, Information, physics and computation. Oxford Graduate Texts. 2009.
- A.H. Lang et al., Epigenetic Landscapes Explain Partially Reprogrammed Cells and Identify Key Reprogramming Genes. PLOS Comp Biol. Vol. 10(8): e1003734 (2014)
- Hopfield, J. J. Neural networks and physical systems with emergent collective computational abilities. Proc. Natl. Acad. Sci. U.S.A. 79 (8): 2554–2558. (1982)
- D.J. Evans and D.J. Searles. The Fluctuation theorem. Adv. Phys. 51(7):1529-85 (2002)
- Y.I. Wolf et al., Physical foundations of biological complexity. PNAS, 2018
- B Derrida and H Spohn, Polymers on disordered trees, spin glasses and travelling waves. J. Stat. Phys. 51 (516): 1988
- Turing, A.M. The chemical basis of morphogenesis. Philos. Trans. R. Soc. Lond. B: Biol. Sci. 237 (641): 37–72 (1952)
- Fisher, R.A. The wave of Advance of Advantageous Genes. Annals of Eugenics. 7(4):353-369 (1937)
- Kolmogorov, A., Petrovskii, I. & Piskunov, N. Study of the diffusion equation with growth of the quantity of matter and its application to a biological problem. Bull. State Univ. Mos., 1-25. (1937)
- Gatenby, RA and Gawlinki. A reaction-diffusion model of cancer invasion. Cancer Research 56(24):5745-53 (1996)

- Ramis-Conde, I. et al. Mathematical modelling of cancer cell invasion of tissue. Math. Comp. Modelling. 47(5-6):533-545 (2008)
- P. Domsuhke et al. JTB. 361:41-60 (2014)- Mathematical modelling of cancer invasion: implications of cell adhesion variability for tumor infiltrative growth patterns
- Cooke J, Zeeman EC. A clock and wavefront model for control of the number of repeated structures during animal morphogenesis. J Theor Biol. 58(2):455-76. (1976)
- Wolpert, L. Positional information and the spatial pattern of cellular differentiation. J. Theor. Biol. 25 (1), 1–47 (1969)
- Laurence Garric & Jeroen Bakkers , Shaping up with morphogen gradients. *Nature Cell Biology*. 20, 998–999 (2018)
- Lauschke, V.M. et al. Scaling of embryonic patterning based on phase-gradient encoding. Nat. 493:101-106 (2013)
- Green, J.B.A and Sharpe, J. Positional information and reaction-diffusion: two big ideas in developmental biology combine. Development 2015 142: 1203-1211
- Battle, E., & Clevers, H., Cancer stem cells revisited. Nat Med. 23(10):1124-1134 (2017)
- M. Pascaal, Diffusion-induced chaos in a spatial predator-prey system. Roy Soc. Proc. Biol. Sci. 251:1330 (1-7) (1993)
- Cai Y, Wu J, Li Z, Long Q (2016) Mathematical Modelling of a Brain Tumour Initiation and Early Development: A Coupled Model of Glioblastoma Growth, Pre-Existing Vessel Co-Option, Angiogenesis and Blood Perfusion. PLoS ONE 11(3): e0150296.
- P.M. Altrock, the mathematics of cancer: integrating quantitative models. Nat Rev cancer. 15:730-745 (2015)
- Weis, Jared A et al. “Predicting the Response of Breast Cancer to Neoadjuvant Therapy Using a Mechanically Coupled Reaction-Diffusion Model.” *Cancer research* vol. 75,22 (2015): 4697-707.
- Jarrett, Angela M et al. “Incorporating drug delivery into an imaging-driven, mechanics-coupled reaction diffusion model for predicting the response of breast cancer to neoadjuvant chemotherapy: theory and preliminary clinical results.” *Physics in medicine and biology* vol. 63,10 105015. (2018)
- T. Harko and M.K. Mak, Travelling wave solutions of the reaction-diffusion mathematical model of Glioblastoma growth: an abel equation based approach. Mathematical Biosciences and Eng. 12(1) (2015)
- Yan, H. et al. 3D Mathematical Modeling of Glioblastoma Suggests That Transdifferentiated Vascular Endothelial Cells Mediate Resistance to Current Standard-of-Care Therapy. Cancer Res; 77(15) (2017)
- Zheng Q, Shen J, Wang Z (2018) Pattern dynamics of the reaction-diffusion immune system. PLoS ONE 13(1): e0190176.
- T Hoshino et al., Pattern formation of skin cancers: effects of cancer proliferation and hydrodynamic interactions. Phys Rev. E 99, 032416 (2019)
- Jose Negrete, Jr. and Andrew C. Oates. Embryonic lateral inhibition as optical modes: An analytical framework for mesoscopic pattern formation. Phys. Rev. E 99, 042417 (2019)
- Mackey, M. C. and Glass, L. (1977). Oscillation and chaos in physiological control systems. Science, 197 (4300): 287-289

- O. E. Rössler, Chaotic behavior in simple reaction system, *Zeitschrift für Naturforsch A*, 31, 259-264, 1976
- Computation of bifurcation diagrams for Selkov's model of glycolytic oscillations. In L. Rensing and N. I. Jaeger (eds.): Temporal Order, pp. 197-200. Berlin: Springer, 1985
- M.L. Heltberg et al., On chaotic dynamics in transcription factors and the associated effects in differential gene regulation. *Nature Communications* 10, Article number: 71 (2019)
- M. Itik. & S.P. Banks. Chaos in a three-dimensional cancer model. international Journal of bifurcation and chaos. 20(01):71 -79 (2010)
- T.T. Ivancevic et al. A theoretical model of chaotic attractor in tumor growth and metastasis. arXiv:0807.4272 (2008) [q-Bio]
- Lorenz, E.N. Deterministic nonperiodic flow. J. Atm. Sci. 20:130-141 (1963)
- A.C. Newell and J. A. Whitehead, J. Fluid Mech. 38 (1969): 279
- E.M. Posadas et al. Chaotic oscillations in cultured cells: rat prostate cancer. Cancer Res. 1996
- Khajanchi, S. et al. The influence of time delay in a chaotic cancer model. Chaos 28, 103101 (2018)
- V. Briane, et al. Statistical analysis of particle trajectories in living cells. Phys. Rev. E 97, 062121 (2018)
- C. Letellier et al. What can be learned from a chaotic cancer model? J. Theor. Biol. 322: 7-16 (2013)
- Yankeelov, Thomas E et al. “Toward a science of tumor forecasting for clinical oncology.” *Cancer research* vol. 75,6 (2015): 918-23.
- Yankeelov, Thomas E et al. “Clinically relevant modeling of tumor growth and treatment response.” *Science translational medicine* vol. 5,187 (2013)
- Tang, L. et al. (2014) Computational Modeling of 3D Tumor Growth and Angiogenesis for Chemotherapy Evaluation. PLoS ONE 9(1): e83962.
- P Hou et al. Pluripotent stem cells induced from mouse somatic cells by small molecule compounds, Science. 341 (6146) (2013)
- C Hernandez et al., Dppa2/4 facilitate epigenetic remodelling during reprogramming to pluripotency. Cell Stem Cell. 23, 396-411 (2018)
- I Kogut et al. High efficiency RNA based reprogramming of human primary fibroblasts. Nat Comm. 9, 745 (2018)
- Rais, X. et al. Nat. 3:502 (7469):65-70 (2013) Deterministic direct reprogramming of somatic cells to pluripotency
- C.L. Barker and M.F. Pera, Capturing Totipotent stem cells. Cell Stem Cell. 22(1):25-34 (2018)
- F. Etoc and A. Brivanlou, A boost towards totipotency for stem cells. Nature Cell Biology 21, 671–673 (2019)
- Macarlan, T.S. et al. Embryonic stem cell potency fluctuates with endogenous retrovirus activity, Nature, 457(7405):57-63 (2012)
- S. Ranquist et al. Algorithm for cellular reprogramming, PNAS, 114(45): 11832-37 (2017)
- T. Zhao et al. Single-Cell RNA-Seq Reveals Dynamic Early Embryonic-like Programs during Chemical Reprogramming. Cell Stem Cell, 23(1): 31-45 (2018)
- Smith, Rosanna C G et al. “Nanog Fluctuations in Embryonic Stem Cells Highlight the Problem of Measurement in Cell Biology.” Biophysical journal vol. 112,12 (2017): 2641-2652.

- J.C. Yin et al. chemical conversion of human fetal astrocytes into neurons through modulation of multiple signaling pathways. Stem Cell Reports, 12:1-14 (2019)
- O'Brien-Ball, C. & Biddle, A. Reprogramming to developmental plasticity in cancer cells. Dev Biol. 430(2):266-274 (2017)
- K.M. Haigis et al. Tissue-specificity in cancer: the rule, not the exception. Science. 363: 6432. Pp. 1150-1151 (2019)
- Kim J et al. A Myc network accounts for similarities between embryonic stem cell and cancer cell transcription programs. Cell. 2010. 143:313-324.
- Yan, Wei et al. Cancer-cell-secreted exosomal miR-105 promotes tumour growth through the MYC-dependent metabolic reprogramming of stromal cells. Nature cell biology vol. 20,5 (2018)
- E. Wingrove et al. Transcriptomic hallmarks of tumor plasticity and stromal interactions in brain metastases, Cell Reports, 27(4):1277-1292 (2019)
- Duman, C. et al. Acyl-CoA-Binding protein drives glioblastoma tumorigenesis by sustaining fatty acid oxidation. Cell Metabolism (2019)
- A. Dirkse et al., Stem cell-associated heterogeneity in Glioblastoma results from intrinsic tumor plasticity shaped by the microenvironment. Nat. Comm. 10: 1787 (2019)
- Patel, A. P et al. “Single-cell RNA-seq highlights intratumoral heterogeneity in primary glioblastoma.” Science (New York, N.Y.) vol. 344,6190 (2014): 1396-401.
- Yuan, Jinzhou et al. “Single-cell transcriptome analysis of lineage diversity in high-grade glioma.” Genome medicine vol. 10,1 57. 2018
- Charles P. Couturier et al., Single-cell RNA-seq reveals that glioblastoma recapitulates normal brain development. BioRxiv. doi: https://doi.org/10.1101/449439 (2018)
- Suvà, M.L. et al. Epigenetic Reprogramming in Cancer. Science 339.6127 (2013)
- Suva, ML. et al. Reconstructing and reprogramming the tumor propagating potential of glioblastoma stem-like cells; Cell. 157(3): 580–594. (2014)
- Bago, J.R. et al. Tumor-homing cytotoxic human induced neural stem cells for cancer therapy. Science Trans. Med. Vol. 9, Issue 375, eaah6510 (2017)
- Z. Wang et al. Methionine in is a metabolic dependency of tumor initiating cells. Nat Med, 25, 825 -837 (2019)
- Malladi, Srinivas et al. “Metastatic Latency and Immune Evasion through Autocrine Inhibition of WNT.” Cell vol. 165,1 (2016): 45-60.
- Gold, P. & Freedman, S.O. Specific carcinoembryonic antigens of the human digestive system. J Exp Med. 122(3):467-81. (1965)
- Y. Guo et al. Effects of exosomes on pre-metastatic niche formation in tumors. Molecular Cancer. 18:39 (2019)
- Wei-xian, Chen et al., Exosomes from drug resistant breast cancer cells transmit chemoresistance by a horizontal transfer of microRNAs. PLoS One 9(4): e95240 (2014)
- Hu, Y. et al. Fibroblast derived exosomes contribute to chemoresistance through priming cancer stem cells in colorectal cancer. PLoS One 10(5): e0125625 (2015)
- Zhang, C. et al. “Exosome: Function and Role in Cancer Metastasis and Drug Resistance.” Technology in cancer research & treatment vol. 17 (2018): 1533033818763450.
- Costa-Silva, Bruno et al. “Pancreatic cancer exosomes initiate pre-metastatic niche formation in the liver.” Nature cell biology vol. 17,6 (2015): 816-26.

- Lane, R E et al. “Extracellular vesicles as circulating cancer biomarkers: opportunities and challenges.” *Clinical and translational medicine* vol. 7,1 14. (2018)
- Huang, Tao, and Chu-Xia Deng. “Current Progresses of Exosomes as Cancer Diagnostic and Prognostic Biomarkers.” *International journal of biological sciences* vol. 15,1 1-11. (2019)
- S. Garcia-Silva et al. Use of extracellular vesicles from lymphatic drainage as surrogate markers of melanoma progression and BRAFv600E mutation. J. Exp Med.1061-1070 (2019)
- Figueroa, Javier M et al. “Detection of wild-type EGFR amplification and EGFRvIII mutation in CSF-derived extracellular vesicles of glioblastoma patients.” *Neuro-oncology* vol. 19,11 (2017)
- Choi, D. et al. The Impact of Oncogenic EGFRvIII on the Proteome of Extracellular Vesicles Released from Glioblastoma Cells. Mol Cell Proteomics. 17(10):1948-1964 (2018)
- Guo, Deliang et al. “Lipid metabolism emerges as a promising target for malignant glioma therapy.” CNS oncology vol. 2,3 (2013): 289-99.
- Martinelli, Paola et al. “GATA6 regulates EMT and tumour dissemination, and is a marker of response to adjuvant chemotherapy in pancreatic cancer.” Gut vol. 66,9 (2017): 1665-1676
- Dart, A., CXCR2-targeted therapy for pancreatic cancer. Nat Rev Cancer. Nature Reviews Cancer volume 16 (2016)
- Zhao, Lu et al. “Verapamil inhibits tumor progression of chemotherapy-resistant pancreatic cancer side population cells.” International journal of oncology vol. 49,1 (): 99-110. (2016)
- S.T. Chao et al. Imaging extracellular vesicles: current and emerging methods. J Biomed Sci. 25:91 (2018)
- F.J. Verweij et al., Quantifying exosome secretion from single cells reveals a modulatory role for GPCR signaling. JCB 2018
- Lai, C.P. et al. Visualization and tracking of tumour extracellular vesicle delivery and RNA translation using multiplexed reporters. Nat Comm. 2015
- Lai, CP. Et al. Dynamic biodistribution of extracellular vesicles in Vivo using a multimodal imaging reporter. ACS nano, 8(1):483-94 (2014)
- P. Gangadaran et al., An update on in Vivo imaging of extracellular vesicles as drug delivery vehicles. 2018
- Skog J, Wurdinger T, van Rijn S, et al. Glioblastoma microvesicles transport RNA and proteins that promote tumour growth and provide diagnostic biomarkers. Nat Cell Biol. 2008
- Sinha MS et al. Alzheimer’s disease pathology propagation by exosomes containing toxic amyloid-beta oligomers. Acta Neuropathol. 136(1): 41–56. (2018)
- Camussi, G. et al. Exosome/microvesicle-Mediated Epigenetic Reprogramming of Cells. American Journal of Cancer Research 1.1: 98–110 (2011)
- Zhou, Shufeng et al. “Reprogramming Malignant Cancer Cells toward a Benign Phenotype following Exposure to Human Embryonic Stem Cell Microenvironment” PloS one vol. 12,1 e0169899. (2017)
- Abdouh, M. et al. Exosomes isolated from cancer patients’ sera transfer malignant traits and confer the same phenotype of primary tumors to oncosuppressor-mutated cells, Journal of Experimental & Clinical Cancer Research. 36:113 (2017)

- Leal, A.C. et al., Tumor-Derived Exosomes Induce the Formation of Neutrophil Extracellular Traps: Implications For The Establishment of Cancer-Associated Thrombosis. Scientific Reports 7, Article number: 6438 (2017
- Hwang, Wei-Lun et al. "Tumor stem-like cell-derived exosomal RNAs prime neutrophils for facilitating tumorigenesis of colon cancer." Journal of hematology & oncology vol. 12,1 10. 25 Jan. 2019
- P Yang et al. Multiomic profiling reveals dynamics of the phased progression of pluripotency. Cell systems, 2019.
- C. Le Toumeau et al. Molecular profiling in precision medicine oncology. Nat med. 25, 711-712 (2019)
- J. Rodon et al. Genomic and transcriptomic profiling expands precision cancer medicine: the WINTHER trial. Nat Med. 25, 751-758 (2019)
- Kopper et al. An organoid platform for ovarian cancer captures intra- and interpatient heterogeneity. Nat Med. 2019
- G. Lemoult et al. Directed percolation phase transition to sustained turbulence in Couette flow. *Nature Physics* volume12, pages254–258 (2016)
- T.R.J. Bossamaier and D.G. Green, Complex Systems. Cambridge Univ. Press, 2000
- Esteva, A. et al. A guide to deep learning in healthcare. Nat. Med 25, pages24–29 (2019)
- *E. J. Topol, High Performance medicine: the convergence of human and artificial intelligence. Nat Med. 25, 44-56 (2019)*
- D. Silverbush et al. Simultaneous interpretation of multi-omics data improves the identification of cancer driver modules. Cell Systems, 2019.
- P. Yang et al., Multi-omic Profiling Reveals Dynamics of the Phased Progression of Pluripotency. Cell Systems 8, 427–445 (2019)
- *LeCun, Y., Bengio, Y. and Hinton, G. Deep learning. Nature 521: 436-444 (2015)*
- *Shan, H. et al.* Competitive performance of a modularized deep neural network compared to commercial algorithms for low-dose CT image reconstruction. *Nature Machine Intelligence.* volume 1, pages269–276 (2019)
- Zhang, Z. et al. Pathologist-level interpretable whole-slide cancer diagnosis with deep learning. *Nature Machine Intelligence.* volume 1, pages236–245 (2019)
- Lennon FE et al., Lung cancer- a fractal viewpoint. Nat Rev Clin Oncol. 12(11): 664–675. (2015)
- Bolhaquiero, A.C.F. et al. Ongoing chromosomal instability and karyotype evolution in human colorectal cancer organoids. Nature Genetics 51, 824–834 (2019)
- Wangsa, D. et al. Near-tetraploid cancer cells show chromosome instability triggered by replication stress and exhibit enhanced invasiveness. The FASEB Journal 32(7):fj.201700247RR (2018)
- Tong, W. and Altman, R.B. High precision protein functional site detection using 3D convolutional neural networks. Bioinformatics, 35(9):1503-1512 (2009)
- A.T. Fard and M.A. Ragan, modelling the attractor landscape of disease progression: a network-based approach. Front Genetics (2017)
- C. G. Palii et al. Single-cell proteomics reveal that quantitative changes in co-expressed lineage-specific transcription factors determine cell fate. Cell Stem Cell, 24(5): 812-820 (2019)

- Zhao, Lan et al. “Gene expression profiling of 1200 pancreatic ductal adenocarcinoma reveals novel subtypes.” *BMC cancer* vol. 18,1 603. 29 (2018)
- Z. Castello and H.G. Martin, A machine learning approach to predict metabolic pathway dynamics from time-series multiomics data. Npj syst Biol. App. 4:19 (2018)
- H Li et al. The landscape of cancer cell line metabolism. Nat Med. 25, 850-860 (2019)
- Krieger, M.S. et al. Novel cytokine interactions identified during perturbed hematopoiesis. BioRxiv, 2018. http://dx.doi.org/10.1101/484170.
- J. N. Kather et al. Deep Learning can predict microsatellite instability directly from histology in gastrointestinal cancer. Nat Med. 2019
- Zhe Shun et al., A Bayesian mixture model for clustering droplet-based single-cell transcriptomic data from population studies. Nat Comm. 10:1649 (2019)
- W Saelens et al. A comparison of single-cell trajectory inference methods. Nat Biotech. 37, 547-554 (2019)
- Chan et al., Gene regulatory network inference from single cell data using multivariate information measures. Cell Systems 5, 251-267 (2017)
- G. L. Stein-O’Brien et al., Decomposing Cell Identity for Transfer Learning across Cellular Measurements, Platforms, Tissues, and Species. Cell Systems 8, 395–411 (2019)
- *Y.T. Lin et al., A stochastic and dynamical view of pluripotency in mouse embryonic stem cells. PLoS Comput Biol. 14(2): e100600 (2018)*
- *P.S. Stumpf et al., Stem cell differentiation as a non-Markov stochastic process. Cell Systems 5, 268-282 (2017)*
- Zwiessele, M. and Lawrence, N.D. Topslam: Waddington Landscape Recovery for Single Cell Experiments. BioRxiv doi: https://doi.org/10.1101/057778 (2017)
- Lummertz da Rocha, E., et al. Reconstruction of complex single-cell trajectories using CellRouter. Nature Comm. 9: 892 (2018)
- A Butler et al. Integrating single-cell transcriptomic data across different conditions, technologies and species. Nat biotech. 36, 411-420 (2018)
- Jin S et al., scEpath: energy landscape-based inference of transition probabilities and cellular trajectories from single-cell transcriptomic data. Bioinformatics, 34(12):2077-2086 (2018)
- K. Street et al. Slingshot: cell lineage and pseudotime inference for single-cell transcriptomics. BMC Genomics, 19:477 (2018).
- Szedlak et al. Control of asymmetric Hopfield networks and application to cancer attractors. PLoS ONE 9(8): e105842 (2014)
- Lin, C et al. Using neural networks for reducing the dimensions of single-cell RNA-Seq data. *Nucleic Acids Research*, Volume 45, Issue 17. (2017)
- J. Guo and J. Zheng, Hopland: single cell pseudotime recovery using continuous Hopfield network-based modelling of Waddington’s epigenetic landscape. Bioinformatics, 33(14): i102-109 (2017)
- J Guo et al., NetLand: quantitative modelling and visualization of Waddington’s epigenetic landscape using probabilistic potential. Bioinformatics, 33(10):1583-1585 (2017)
- Tian, T. et al. Clustering single-cell RNA-seq data with a model-based deep learning approach. *Nature Machine Intelligence.* volume 1, pages191–198 (2019)

- K. Gustafson, Graph theory in the approximation theory of fluid dynamics. Ann. Vol. Approx. Theory and Functional Analysis. 511-519. Int Ser of Numerical Mathematics. Vol. 65 (1984)
- K. Gustafson and R. Hartman, Graph theory and fluid dynamics. SIAM J. Alg. Disc. Meth. 6(4):1985
- J. Takeuchi and Y. Kosugi, Neural network representation of finite element method. Neural networks. 7(2):389-395 (1994)
- S. Chen and G.D. Doolen. Lattice Boltzmann method and fluid flows- Ann Rev. Fluid Mech. 30: 329-64 (1998)
- A Farsikov et al. Optimal Control problems for the Navier-Stokes equations. Lect Appl. Math. Pp 143-155 (2000)
- Q. Li et al. Hyperchaos in Hopfield-type neural networks. Neurocomputing, vol. 67: 275-280 (2005) 0 with 4 neurons
- S Yang and Y Huang. Complex dynamics in simple Hopfield neural networks. Chaos 16, 033114 (2016)
- Jeremy, M. et al. Intraoperative brain cancer detection with Raman spectroscopy in humans. Sci Transl Med. 7(274):274ra19 (2015)
- Brusatori, M. et al. Intraoperative Raman Spectroscopy. Neurosurg Clin N Am. 28(4):633-652 (2017)
- Zhao, J. et al. Automated Autofluorescence Background Subtraction Algorithm for Biomedical Raman Spectroscopy. Applied Spectroscopy. 61(11): 1225-1232 (2007)
- Gualerzi, Alice et al. “Raman spectroscopy uncovers biochemical tissue-related features of extracellular vesicles from mesenchymal stromal cells” Scientific reports vol. 7,1 9820. (2017)
- Gualerzi, A. et al. Raman spectroscopy as a quick tool to assess purity of extracellular vesicle preparations and predict their functionality. Journal of Extracellular Vesicles, 8:1, 1568780, (2019)
- Shin H, Correlation between Cancerous Exosomes and Protein Markers Based on Surface-Enhanced Raman Spectroscopy (SERS) and Principal Component Analysis (PCA). *ACS Sens.*, 2018, *3* (12), pp 2637–2643
- Ko, Jina et al. “Detection and isolation of circulating exosomes and microvesicles for cancer monitoring and diagnostics using micro-/nano-based devices.” *The Analyst* vol. 141,2 (2016): 450-460.
- Banaei, N. et al. Multiplex detection of pancreatic cancer biomarkers using a SERS-based immunoassay. Nanotechnology. 2017 Nov 10;28(45):455101
- K. Yizhak et al. RNA Sequence analysis reveals macroscopic somatic clonal expansion across normal tissues. Science, 364: 6444, eaaw0726 (2019)
- Arts & Culture: Turbulence in *The Starry Night. APS Physics.* April 18, 2019• *Physics* 12, 45. https://physics.aps.org/articles/v12/45
- Wensink, Henricus H et al. Meso-scale turbulence in living fluids. PNAS, 109(36): 14308-13 (2012)
- Hong-Yan Shih et al. Ecological collapse and the emergence of travelling waves at the onset of shear turbulence. Nat. Phys. Vol 12: 245-248 (2016)
- D. Ruelle, Strange attractors. Math. Intelligencer, vol 2: 126-137 (1980)
- Ruelle, D. Turbulence, strange attractors and chaos. World Scientific Ser A. 16. (1995)

- A Brandstater and HL Swinney, Strange attractors in weakly turbulent Couette-Taylor flow. Phys Rev A. 35(5):2207-2220 (1987)
- The strange attractor theory of turbulence. O.E. Lanford III, Ann rev Fl Mech. 14:347-364 (1982)
- J Miles Strange attractors in fluid dynamics. Adv App. Math. 24: 189-214 (1984)
- J. Leray. Sur le mouvement dun liquide visqueux emplissant lespace, Acta Math. 63 (1934), 193248
- Kolmogorov, A. N. Dissipation of energy in locally isotropic turbulence [Russian]. *Dokl. Akad. Nauk SSSR* 32, 16–18 (1941); English translation available in Levin, V. *Proceedings: Mathematical and Physical Sciences (Turbulence and Stochastic Process: Kolmogorov's Ideas 50 Years On)* Vol. 434 15–17 (Royal Society, 1991)
- Nigel Goldenfeld, Roughness-Induced Critical Phenomena in a Turbulent Flow. PRL 96, 044503 (2006)
- V. I Arnold and BA Khesin, Topological methods in hydrodynamics. Springer 1991
- R.L. Rico (2000) An introduction to the geometry and topology of fluid flows. Kluwer Academic Publishers.
- Tao, T. Searching for singularities in the Navier-Stokes equations. Nat Rev Phys. (2019)
- J.N. Kutz, Deep learning in fluid dynamics. J. Fluid Mech. 814:1-4 (2017)
- Brunton, S.L. et al., Machine Learning for Fluid Mechanics. arXiv:1905.11075v1 [physics.flu-dyn] 27 May 2019
- S.D. Sarma et al. Machine learning meets quantum physics. Physics Today, 72(3): 48 (2019)
- D. Ruelle, Some comments on chemical oscillations. Trans NewYork Acad. Sciences, Ser II. 35(1):66-71 (1973)
- D. Ruelle and F Takens. On the nature of turbulence. Commun Multi Phys. 20, 167-192 (1971)
- Brauns, F., Halatek, J. and Frey, E. Phase-space geometry of reaction-diffusion dynamics. arXiv:1812.08684 [nlin.PS] (2018)
- David P. Ruelle. Hydrodynamic turbulence as a problem in nonequilibrium statistical mechanics. PNAS 109 (50) 20344-20346 (2012)
- D. Ruelle, Nonequilibrium statistical mechanics of turbulence. J Stat Phys. 157(2), 205-208 (2014)
- Hojin, H. et al. Age-Related Vascular Changes Affect Turbulence in Aortic Blood Flow. *Frontiers in physiology* vol. 9:36. (2018)
- Ito, Y., et al. Turbulence activates platelet biogenesis to enable clinical scale ex vivo production. Cell. 174(3): 636-648 (2018)
- Koumoutsakos, P. et al. The fluid mechanics of cancer and its therapy. Ann. Rev. Fl. Mech. 45:325-355 (2013)
- Goetz JG, Metastases go with the flow. Science 362(6418):999-1000 (2018)
- Thamilselvan V, Basson MD. Pressure activates colon cancer cell adhesion by inside-out focal adhesion complex and actin cytoskeletal signaling. Gastroenterology. 2004;126(1):8–18
- Chivukula, Venkat Keshav et al. "Alterations in cancer cell mechanical properties after fluid shear stress exposure: a micropipette aspiration study". *Cell health and cytoskeleton* vol. 7 (2015): 25-35.

- Rizvi, Imran et al. “Flow induces epithelial-mesenchymal transition, cellular heterogeneity and biomarker modulation in 3D ovarian cancer nodules.” *Proceedings of the National Academy of Sciences of the United States of America* vol. 110,22 (2013): E1974-83.
- Ketene AN et al. The effects of cancer progression on the viscoelasticity of ovarian cell cytoskeleton structures. Nanomedicine. Jan;8(1):93-102 (2012)
- Huang, Q et al. Fluid shear stress and tumor metastasis. *American journal of cancer research* vol. 8,5 763-777. (2018)
- J. W. Baish and R.K. Jain, Fractals and cancer. Canc. Res 60:3683-3688 (2000)
- R. Nasu et al. Blood flow influences vascular growth during tumor angiogenesis. British Journal of Cancer (1999) 79(5/6), 780–786
- Sreenivasan, K.R. and Meneveau, C. The fractal facets of turbulence. J Fluid Mech. Vol. 173: 357-386 (1986)
- Sreenivasan, K.R. and Meneveau, C. The multifractal nature of turbulent energy dissipation. J. Fluid Mech. Vol 224: 429-484 (1991)
- Coffey, WT. Self-organization, complexity and chaos: The new biology for medicine. Nat
- Med. 4(8): 882-885 (1998)
- Victor Yakhota and K.R. Sreenivasan, Towards a dynamical theory of multifractals in turbulence. Physica A 343 (2004) 147–155
- Rejniak, Katarzyna A. “Circulating Tumor Cells: When a Solid Tumor Meets a Fluid Microenvironment.” Advances in experimental medicine and biology vol. 936 (2016): 93-106.
- Behr, Julie et al. “Localized Modeling of Biochemical and Flow Interactions during Cancer Cell Adhesion.” *PloS one* vol. 10,9 e0136926. (2015)
- Yasuhara K et al. 25(4):183-8. New color Doppler technique for detecting turbulent tumor blood flow: a possible aid to hepatocellular carcinoma diagnosis. J Clin Ultrasound. (1997)
- Kalgin, I.V. & Chekmarev, S.F. Turbulent phenomena in protein folding. Phys Rev E. 83, 011920 (2011)
- Andryushchenko, V.A. & Chekmarev, S.F. Turbulence in protein folding: Vorticity, scaling and diffusion of probability flows. PLoS One. 12(12): e0188659 (2017)
- V. A. Andryushchenko and S. F. Chekmarev,, On hydrodynamic interpretation of folding of an α-helical protein. Thermophysics and Aeromechanics. Volume 23, Issue 6, pp 941–944 (2016)
- S. F. Chekmarev, Protein Folding Dynamics in the Space of Experimentally Measured Variables: Turbulence Phenomena. J App Mech. Techn. Phys. Vol. 59, Issue 5, pp 827–833 (2018)
- Dunkel J et al. Fluid dynamics of bacterial turbulence. Phys Rev Lett. 110(22):228102 (2013)
- *Martinez-Pratt et al. Selection mechanism at the onset of active turbulence. Nature Physics, 15:362-366. (2019)*
- Y. Sumino et al. "Large-scale vortex lattice emerging from collectively moving microtubules". *Nature*. 483 (7390): 448–452 (2012)
- Marchetti, M.C. et al. Hydrodynamics of soft active matter. Rev Mod Phys. 85(3) (2013)
- A.W. Baggaley, Stability of model flocks in a vortical flow. Phys. Rev. E 93, 063109 (2016)
- M. James, W.J.T. Bos, M. Wilczek, Turbulence and turbulent pattern formation in a minimal model for active fluids, Phys Rev. Fluids 3, 061101(Rapid Communication) (2018)
- M. James, M. Wilczek, Vortex dynamics and Lagrangian statistics in a model for active turbulence, EPJE 41, 21 (2018)

- P. Gross et al. Guiding self-organized pattern formation in cell polarity establishment. *Nature Physics* 15, 293–300 (2019)
- Doostmohammadi et al. Active nematics, *Nature Communications.* Volume 9, Article number: 3246 (2018)
- Halatek, J. & Frey, E. Rethinking pattern formation in reaction–diffusion systems. *Nat. Phys.* 14: 507-514 (2018) doi:10.1038/s41567-017-0040-5
- J. Denk, et al., MinE conformational switching confers robustness on self-organized Min protein patterns. PNAS, 115 (18) 4553-4558. (2018).
- Kim, M. et al. Controlling Chemical Turbulence by Global Delayed Feedback: Pattern Formation in Catalytic CO Oxidation on Pt (110). Science. Vol. 292, Issue 5520, pp. 1357-1360 (2001)
- K. R. Mecke. Morphological characterization of patterns in reaction-diffusion systems. Phys. Rev. E 53, 4794 (1996)
- Q Ouyang and H.L. Swinney, transition to chemical turbulence. Chaos, 1991. 1, 411
- Helbing D, et al. Dynamics of crowd disasters: An empirical study. Phys. Rev. E 75, 046109 (2007)
- Lambert, N., et al. Quantum Biology. Nature Phys. 9:10-18 (2012)
- Hameroff, S., Penrose, R. Consciousness in the universe: a review of the 'Orch OR' theory. Phys. Life Rev. 11 (1), 39–78. (2014)
- L. Shaedel et al. Lattice defects induce microtubule self-renewal. Nat Phys 2019
- Lens, S.M.A & R.H. Medema, R.H. Cytokinesis defects and cancer, *Nature Reviews Cancer.* 19:
- 32–45 (2019)
- Marais, Adriana et al. "The future of quantum biology." *Journal of the Royal Society, Interface* vol. 15,148 20180640. 14 Nov. 2018
- McFadden, Johnjoe, and Jim Al-Khalili. "The origins of quantum biology." *Proceedings. Mathematical, physical, and engineering sciences* vol. 474,2220 (2018)
- Engel G.S. et al., Evidence of wavelike energy transfer through quantum coherence in
- photosynthetic systems. Nature, 446 (7137): 782-786 (2007)
- Thyrhaug, E., et al. Identification and characterization of diverse coherences in the Fenna-Matthews–Olson complex, Nat. Chem. 10: 780–786 (2018)
- Craddock TJA, et al. The feasibility of coherent energy transfer in microtubules. J. R. Soc.
- Interface 11: 20140677 (2014)
- Frohlich, H. Long range coherence and energy storage in biological systems. Int. J Quantum
- Chem. 2(5):641-649 (1968)
- Davydov, A.S. Solitons and energy transfer along protein molecules. J. Theor. Biol. 66(2):379-387 (1977)
- Lundholm, I.V. et al. Terahertz radiation induces non-thermal structural changes associated with Frohlich condensation in a protein crystal. Struct. Dyn. 2(5):054702 (2015)
- E. Prodan & C. Prodan. Topological phonon modes and their role in dynamic instability of
- microtubules. Phys Rev Lett. 103(24):248101. (2009)
- Del Giudice, E. et al. A collective dynamics in metabolically active cells. Physica Scripta, 26(3)(1982)
- Marletto, C. *et al.* Entanglement between living bacteria and quantized light witnessed by Rabi
- splitting. *J. Phys. Commun.* 2 101001 (2018)
- Madelung, E. Quantum Theory in Hydrodynamical Form, Z. F. Phys., 40: 322-326 (1927)

- Bohm, D. A suggested interpretation of the Quantum Theory in terms of “hidden variables”. I. Phys. Rev. 85(2):166-179 (1952)
- de Broglie, L. Interpretation of quantum mechanics by the double solution theory. Annales de la Fondation Louis de Broglie, Volume 12, no.4, 1987
- Harvey, R.J. Navier-Stokes analog of Quantum mechanics. Phys Rev 152, 1115 (1966)
- Bohm, D. & Hiley, B. The Undivided Universe: An ontological interpretation of Quantum Theory (Routledge, 1995)
- Bohm, D. Wholeness and the Implicate Order. Routledge, London (1980)
- Andrew W. Baggaley et al. Vortex-Density Fluctuations, Energy Spectra, and Vortical Regions in Superfluid Turbulence. Phys. Rev. Lett. 109, 205304 (2012)
- Holland, P.R. The Quantum theory of motion: an account of de Broglie-Bohm causal interpretation of quantum mechanics. Cambridge Uni Press. (1993)
- Caldeira, A. O and Leggett, A.J. Path integral approach to quantum Brownian motion. Physica A, 121:4857 (1983)
- Jungel, A. et al., A new derivation of the quantum Navier-Stokes equations in the Wigner-Fokker-Planck approach. J. Stat. Phys. 145(6): 1661–1673 (2011)
- Vattay, G., Kauffman, S., & Niiranen, S. Quantum biology on the Edge of Quantum Chaos. PLoS One. 9(3): e89017 (2014)
- G. Vattay *et al.* Quantum criticality at the origin of life. *J. Phys.: Conf. Ser.* 626: 012023. 2015
- Daniel M. Harris *and* John W. M. Bush, The pilot-wave dynamics of walking droplets. Physics of Fluids 25, 091112 (2013)
- Jan Moláček and John W. M. Bush. Drops walking on a vibrating bath: towards a hydrodynamic pilot-wave theory. J Fluid Mech. vol. 727: pp. 612-647 (2013)
- Bush, J.M.W. Pilot-wave hydrodynamics. Ann Rev Fl. Mech. 47:269-292 (2015)

Preprints (www.preprints.org) | NOT PEER-REVIEWED | Posted: 27 June 2019 doi:10.20944/preprints201906.0288.v1

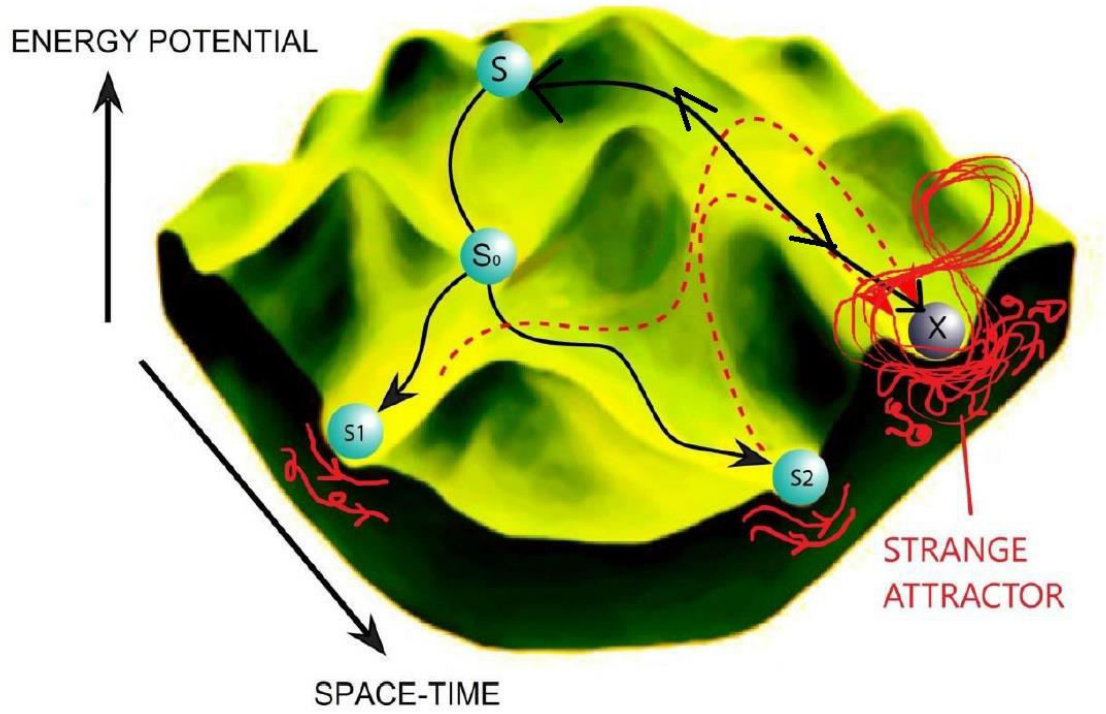

Figure 1: Waddington landscape- The Waddington landscape shows a stem cell S bifurcating to various cell fates represented by the blue balls. As seen in red, the flows of gene expression underlying the differentiated cell states S1 and S2 seem more laminar. However, cell fates are reversible as indicated by the dotted line. Multiple bifurcation routes exist towards a local energy minimum X. The attractor X is a chaotic cell fate (i.e. cancer) and shown as a Lorenz-like strange attractor on the developmental landscape. Note the two-way (revertible) flow from the initial stem cell state to the cancer state.